Science of the Total Environment 543 (2016) 388–404

Contents lists available at ScienceDirect

Science of the Total Environment

journal homepage: www.elsevier.com/locate/scitotenv

Using hysteresis analysis of high-resolution water quality monitoring data, including uncertainty, to infer controls on nutrient and sediment transfer in catchments

C.E.M. Lloyd [a,b,*], J.E. Freer [b], P.J. Johnes [b], A.L. Collins [c]

[a] School of Chemistry, University of Bristol, Cantock's Close, Bristol BS8 1TS, UK
[b] School of Geographical Sciences, University of Bristol, University Road, Bristol BS8 1SS, UK
[c] Sustainable Soils and Grassland Systems Department, Rothamsted Research, North Wyke, Okehampton EX20 2SB, UK

HIGHLIGHTS

- Hysteretic storm behaviour was analysed in 3 water quality parameters at 2 sites
- Storms were analysed within an observational uncertainty framework
- Range of metrics were used, including a new index, to quantify storm hysteresis
- Differences in transport mechanisms shown between nitrate and TP in chalk system.
- Behaviour was complex but provides insight into catchment processes in landscapes.

GRAPHICAL ABSTRACT

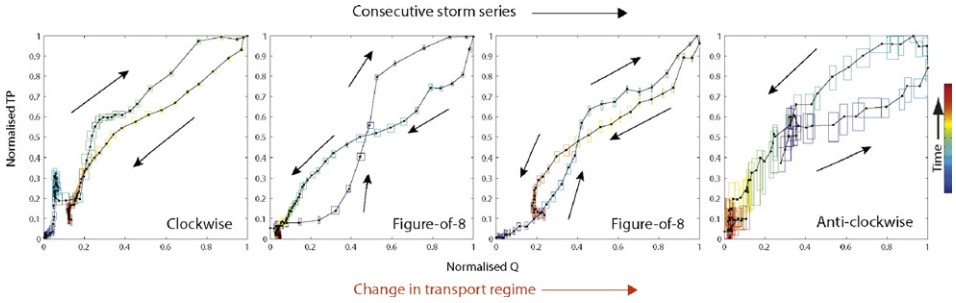

ARTICLE INFO

Article history:
Received 14 September 2015
Received in revised form 5 November 2015
Accepted 5 November 2015
Available online 18 November 2015

Editor: D. Barcelo

Keywords:
Nutrient transport
Storm behaviour
Turbidity
Rivers
Uncertainty
Catchment processes

ABSTRACT

A large proportion of nutrients and sediment is mobilised in catchments during storm events. Therefore understanding a catchment's hydrological behaviour during storms and how this acts to mobilise and transport nutrients and sediment to nearby watercourses is extremely important for effective catchment management. The expansion of available in-situ sensors is allowing a wider range of water quality parameters to be monitored and at higher temporal resolution, meaning that the investigation of hydrochemical behaviours during storms is increasingly feasible. Studying the relationship between discharge and water quality parameters in storm events can provide a valuable research tool to infer the likely source areas and flow pathways contributing to nutrient and sediment transport. Therefore, this paper uses 2 years of high temporal resolution (15/30 min) discharge and water quality (nitrate-N, total phosphorus (TP) and turbidity) data to examine hysteretic behaviour during storm events in two contrasting catchments, in the Hampshire Avon catchment, UK. This paper provides one of the first examples of a study which comprehensively examines storm behaviours for up to 76 storm events and three water quality parameters. It also examines the observational uncertainties using a non-parametric approach. A range of metrics was used, such as loop direction, loop area and a hysteresis index (HI) to characterise and quantify the storm behaviour. With two years of high resolution information it was possible to see how transport mechanisms varied between parameters and through time. This study has also clearly shown the different transport regimes operating between a groundwater dominated chalk catchment versus a surface-water dominated clay catchment. This information, set within an uncertainty framework, means that confidence can be derived that the patterns and relationships thus identified are statistically robust. These

* Corresponding author at: School of Chemistry, University of Bristol, Cantock's Close, Bristol BS8 1TS, UK.
E-mail address: charlotte.lloyd@bristol.ac.uk (C.E.M. Lloyd).

http://dx.doi.org/10.1016/j.scitotenv.2015.11.028

insights can thus be used to provide information regarding transport processes and biogeochemical processing within river catchments.

1. Introduction

Storm events generate significant transport of nutrient fractions and sediment in catchments. A range of publications report that a large proportion of a catchment's annual total phosphorus (TP) load can be transported by a small number of large storm events (Bowes et al., 2003; Evans and Johnes, 2004; Jarvie et al., 2002; Jordan et al., 2007; Verhoff et al., 1979). These are key transport events in which both nutrient and sediment sources are mobilised, releasing pollutants which are transported along flow pathways (surface and subsurface) and delivered to adjacent waters (Beschta, 1987; Evans et al., 2003; Meade and Parker, 1985; Walling and Webb, 1987). Therefore, understanding the role of hydrological activity in storms as a mechanism for the delivery of contaminants to streams is essential for producing effective agricultural land management strategies to support compliance with water quality legislation such as the Water Framework Directive (WFD) (European Parliament, 2000).

The recent expansion of the use of in-situ sensors to monitor nutrient parameters routinely at high temporal resolution is making detailed analysis of catchment behaviours in response to storm flow activation more feasible. Traditionally, parameters such as turbidity have been used to investigate storm behaviours as it can be measured at high frequency and has been shown to be a reasonable surrogate for the transport of sediment and sediment-associated contaminants such as phosphorus (as particulate P), ammonium and particulate organic nitrogen fractions which cannot be measured directly with existing sensor technologies (Grayson et al., 1996; Kronvang et al., 1997; Stubblefield et al., 2007). The more recent introduction of novel sensors systems and bankside automated photometers means that parameters such as nitrate-N and total phosphorus can be investigated at higher temporal resolutions than previously possible.

Understanding of the catchment transport pathways activated during storm events can be enhanced by studying the changing relationship between discharge and water quality parameters during an individual storm event. The relationship often exhibits a cyclical form known as hysteresis. Hysteresis between discharge and suspended sediment or dissolved solids during storm events was first observed by Hendrickson and Krieger (1964) and Toler and Ocala (1965) and since has been noted in many other water quality parameters such as turbidity, nitrate, TP, Total Reactive P (TRP) and conductivity (e.g. Bowes et al., 2009; Carey et al., 2014; House and Warwick, 1998; Lawler et al., 2006).

A paper by Williams (1989) was one of the first studies which described the most common shapes of hysteresis loops and provided possible explanations for why they occur, with respect to suspended sediment concentrations during storm events. Williams (1989) classified hysteresis loops into five classes. Class I was described as a single-valued line, where the increase and decrease in discharge and sediment concentrations are synchronised and suggests this can occur when sediment is plentiful. Class II was a clockwise loop, where the suspended sediment peak concentration occurs early in the discharge event. This is suggested to be caused by quick flushing of sediment which may become exhausted by the end of the storm event. On the other hand, anticlockwise loops (class III) are also common, signifying the sediment peak lagging the discharge. This could provide evidence of differing transit times of water and sediment. Class IV was classified as a mixture of classes I and II, a single-line plus a loop and is described as resulting from a change in the form of the relationship during a storm event, possibly due to sediment availability, storage and transportability. The final class (V) was a figure-of-eight configuration, which combines classes II and III, again caused by a shift in the form of the relationship between discharge and suspended sediment concentration during a single event. It is important to note that many hysteresis loops maybe difficult to classify easily into these classes, and care should be taken with interpretation as the same type of loop could occur for different reasons. Nevertheless, the study of discharge-water quality hysteresis in storm events can provide a valuable research tool to infer the likely contributing source areas and flow pathways contributing to nutrient and sediment transport in catchments.

The examination of hysteresis loops can provide information regarding the time-lags between discharge and contaminants (Drewry et al., 2009; Langlois et al., 2005; Littlewood, 1992). The technique has been widely used over the past two decades in an attempt to increase understanding of how catchments are functioning, for example, Bowes et al. (2005) used the size of hysteresis loops to investigate the TP storage and mobilisation capability of storm events across a reach in the River Swale, Yorkshire during a succession of 10 storms. In addition, Chen et al. (2012) examined hysteresis in inorganic N fraction transport (ammonium, NH_4^+ and nitrate, NO_3^-) for two storms and showed that the transport mechanisms were different between the two parameters. These papers illustrate how catchment responses to storm events are complex and vary between and within catchments, as well as being parameter dependent.

To date, research has generally focussed on a small number of storm events for a particular catchment and often on just one water quality parameter. Against that background, this study is one of the first investigations to examine the storm responses of a range of water quality parameters over a two year period (up to 75 storms), allowing the comparison of storms between catchments with contrasting environmental characteristics, and between differing antecedent conditions and water years. Outram et al. (2014) used hysteresis as a tool to compare one country-wide storm event across three contrasting UK catchments monitored as part of the Demonstration Test Catchment project (McGonigle et al., 2014). The analysis showed interesting differences between catchment behaviours even during similar storm conditions and highlighted the need for a study which directly compares catchments over a broader range of storm events. The second novel aspect of this work is that it examines storm hysteresis accounting for the observational uncertainties in the data records. Krueger et al. (2009) examined uncertainty of storm hysteresis from a modelling perspective and considered four storm events. This study develops this research further and provides a non-parametric approach to quantifying observational uncertainties in both the discharge and water quality parameters and the storm analysis is completed within this uncertainty framework. Previous research has shown that observational uncertainties in these types of data can have implications for routine data analyses to produce data products to underpin catchment management and policy, such as load estimation, even when high temporal resolution data is used (Lloyd et al., 2015b). As a result, using an uncertainty framework in such analyses allows more robust conclusions to be drawn from these complex data sets particularly for when hysteresis behaviour between storms is non-overlapping across uncertainty limits.

This paper uses data from two field sites with contrasting hydrogeology, land use and management in the Hampshire Avon catchment, UK. The Wylye at Brixton Deverill has a groundwater dominated chalk catchment, while the Sem at Prior's Farm has a surface water dominated clay catchment. The catchments lie within 20 km of each other, and both form part of the wider drainage network of the Hampshire Avon catchment. The data were collected as part of the Defra funded

Demonstration Test Catchment programme (McGonigle et al., 2014) and uses high temporal frequency sensor data streams (15–30 min) for discharge, nitrate, and turbidity, and 30 min frequency TP data, with data collected from March 2012 to March 2014. These data are used here to investigate how stormflow hydrochemical transport varies in relation to catchment hydrogeology, rainfall duration and extremes, antecedent conditions, land use or management and season.

2. Methodology

2.1. Site descriptions

The location of the two catchments considered in this study is shown in Fig. 1 and catchment characteristics are shown in Table 1, highlighting the contrasts between the two chosen catchments. Both catchments are located in the headwaters of the Hampshire Avon which is predominantly agricultural with a mix of semi-natural woodland, pasture (rough and improved) and arable land use (Zhang et al., 2012). These catchments were chosen to represent contrasting hydrogeological systems, with the monitoring station at Brixton Deverill influenced by groundwater inputs due to the dominance of chalk geology in the catchment (Allen et al., 2014; Yates and Johnes, 2013) and Prior's Farm hydrology mainly being driven by surface water inputs due to the dominance of clay geology (Allen et al., 2014). Land use in the Wylye catchment is dominated by intensive mixed arable farming, while land use in the Sem catchment is dominated by dairy cattle production (for more details see Table 1). The Brixton Deverill (Wylye) and Prior's Farm (Sem) catchments are 50.22 and 4.97 km^2 and their baseflow indices are 0.93 and 0.23 respectively. Both receive an annual average rainfall total of between 860 and 970 mm (Robson and Reed, 1999).

Table 1
Summary of catchment characteristics.

	Wylye	Sem
Monitoring location	ST 858381	ST891284
Area (km^2)	50.22	4.97
Average rainfall (mm)[a,b]	967	863
Base Flow Index (BFI)[a]	0.93	0.2
Elevation range (m A.S.L.)[a]	125–281	110–190
Average slope (°)[a]	5	2
Monitoring elevation (m A.S.L.)[a]	189	126
Geology	Cretaceous Chalk, Upper Greensand	Clays, greensand
Soil type	Heavy, medium	Heavy, medium, chalk and limestone
Dominant land use	Mixed	Livestock
Arable (%)[c]	49	0
Improved pasture (%)[c]	30	77
Rough grazing (%)[c]	11	14
Woodland (%)[c]	3	6
Urban (%)[c]	7	3

[a] From (Robson and Reed, 1999).
[b] Average 1961–1990.
[c] Based on the ADAS land use database and for reference year 2010 (c.f. Comber et al., 2008).

2.2. Data collection

2.2.1. Discharge data

Discharge data for the Wylye at Brixton Deverill were obtained from the Environment Agency Gauging Station (Gauge number 43,806), which provided 15 min resolution stage height data using a Thistle 24R Incremental Shaft Encoder with a float and counterweight. During periods of modular flow these data were used in conjunction with a stage-discharge curve to calculate discharge (ISO 1100-2, 2010). However, during non-modular flow, the stage heights are used alongside 15 min velocity measurements from a second ultrasonic gauge to calculate discharge using the velocity-area method (ISO 1088, 2007). In the Sem at Prior's Farm, discharge data were collected using a Mace Flow Pro to gain paired stage height and velocity measurements at 15 min temporal resolution to which the velocity-area method was applied (Lloyd et al., 2015b). The measurements were taken within a concrete

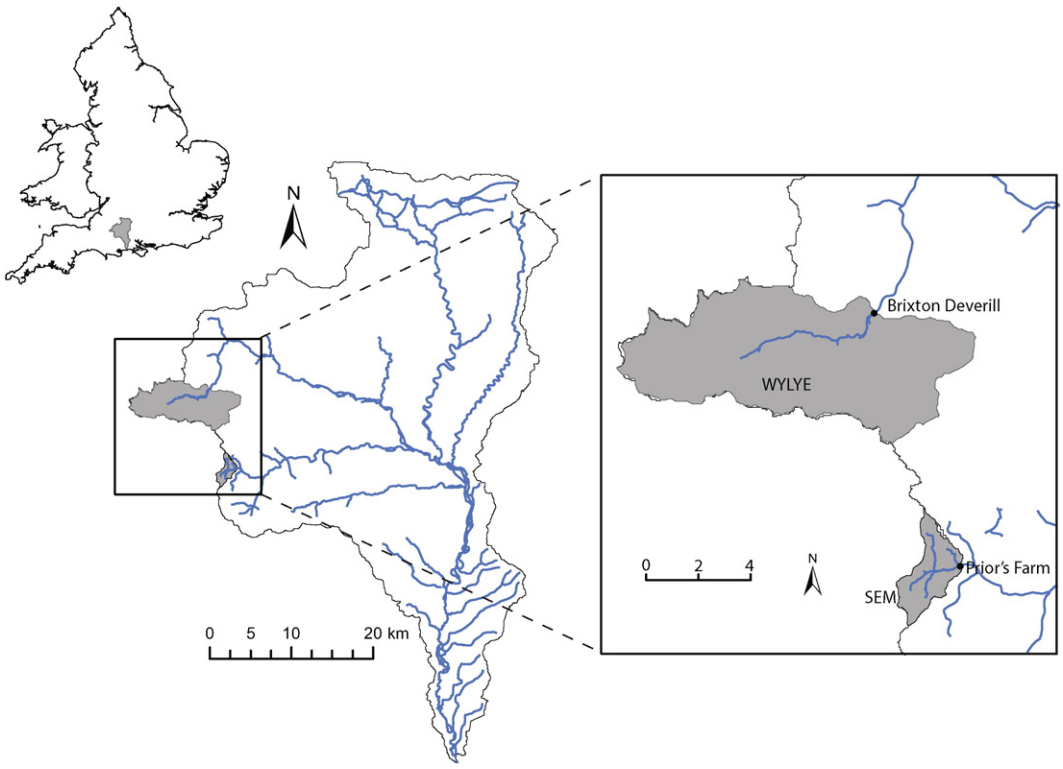

Fig. 1. Map showing the location of the two study catchments in the Hampshire Avon, where the black dots show the monitoring stations.

section which meant that the cross-sectional area was stable. However, during high flow events, the stage height exceeds the height of the concrete structure and out of bank flows occur. In these cases a weir equation was implemented to account for the additional water flowing over the concrete section.

$$Q_i = C_d b H_i^{1.5}$$

where: Q_i is the discharge at time point i ($m^3\ s^{-1}$), C_d is the dimensionless coefficient of discharge, b is the weir crest breadth (m) and H_i is the stage height (m) above the bridge at time point i. C_d was set at 2.7 based on typical values from published literature (Brater and King, 1976).

2.2.2. Water quality data

At both sites, a YSI 6-series sonde was used to measure turbidity optically at 15 min resolution. The probes were cleaned and calibrated once a month to reduce instrument malfunction and drift. In addition, on the Wylye at Brixton Deverill, nitrate-N and total phosphorus (TP) data were collected bankside at 30 min resolution. Nitrate-N data were recorded using a UV optical sensor (Hach Lange Nitratax Plus SC), which was calibrated every three months as recommended by the manufacturer. TP was measured using a wet chemistry analyser (Hach Lange Phosphax Sigma) which uses a colourimetric molybdate method to measure all P compounds as orthophosphate after an acid phase digestion is performed at high temperature and pressure. The instrument was automatically calibrated once a day and the reagents were renewed once every three months, again in line with the recommendations of the manufacturer.

2.3. Quality control and uncertainty analysis

Before further investigation, analysis of all of the data sets was undertaken to quantify the observational uncertainties. A full description of the uncertainty analysis for discharge and nutrient data sets is provided in Lloyd et al. (2015b) but is described briefly below.

2.3.1. Discharge uncertainty

In order to quantify the observational uncertainty in the discharge data, the relationship between stage and calculated discharge at each site was examined. A stable period of this curve was selected in winter (where no or limited shifts in stage-discharge relationships between storms were observed) so that structural changes in the relationship due to seasonal differences in channel characteristics, such as vegetation growth, were not included. Therefore, it was assumed that any noise in the stage-discharge relationship was due to observational uncertainties. A non-parametric local weighted scatterplot smoothing regression (LOWESS) approach was applied to the stable section of the stage-discharge, then a best-fit rating curve was produced and uncertainty bounds determined (Coxon et al., 2015). By examining the residuals from this rating curve, a standard deviation of the residuals could be derived for each stage height, allowing heteroscedasticity to be represented. The degree of autocorrelation in the residual time-series was also examined, but the discharge errors were found in this case to be random. The standard deviation and autocorrelation statistics were then used in a simple 1st-order autoregressive model (Evensen, 2003; Garcia-Pintado et al., 2013; Lloyd et al., 2015b) to simulate 100 iterations of potential error time series (defined as the error model hereafter), which were then added to the original discharge time series to produce 100 deviate data sets. 100 resamples were used because the 10–90th percentiles of the distributions were found to be stable. These 100 data sets are used to represent observational discharge uncertainties in all further analyses in this paper.

2.3.2. Water quality uncertainty

The observational uncertainties associated with the nutrient parameters (nitrate and TP) were quantified by comparing the measured value from the instream sensor with a paired daily sample which was analysed independently in the laboratory using standard digestion and colorimetric analysis (see Lloyd et al. (2015b) for full details). Only samples which were collected within 5 min of each other were used to ensure a robust comparison. The uncertainties in the laboratory samples were also tested using repeated analysis of standard solutions spanning the observed concentrations and the error model was run using variable standard deviations depending on concentration and no temporal autocorrelation to produce 100 iterations of the laboratory derived series. The sensor data were then paired and compared with all 100 iterations of the laboratory time series so that a combined uncertainty was produced. Analysis of the residuals between the laboratory and sensor data showed that they were homoscedastic (not shown), i.e. the variance was not concentration dependent, and that they were autocorrelated. The error model was run accordingly to produce 100 iterations of the sensor data for each of the 100 versions of the laboratory data time series, creating 100,000 versions of the combined sensor data sets, each of which were considered being equally probable. Therefore, for consistency with the discharge data and because the 10–90th percentiles of the distributions were found to be stable after 100 iterations, 100 data sets were randomly sampled from the 100,000 produced. These 100 sensor data sets are used in all further analyses in this study.

In the case of the turbidity, no independent data were available for direct comparison so the variability of the measured turbidity (with individual values representing the average of five recordings per 15 min time step) at times of unchanging discharge (usually baseflow conditions) were used as the best estimate of observational uncertainty. The errors were assumed to be homoscedastic. The residuals were correlated in time and so this information was used to model 100 iterations of the errors and combined with the original time series to produce 100 iterations of the turbidity time series which are used for all further analyses reported here.

2.4. Storm analysis

For the purpose of this analysis, a storm was defined as any hydrological response to rainfall which resulted in a rising and falling limb and where discharge increased by at least 20% of baseflow. Events which had multiple peaks were classified as separate events so that the water quality response to each could be quantified. The discharge data for each storm period was extracted along with the nitrate-N, TP and turbidity data for Brixton Deverill, and turbidity in the case of Prior's Farm. Water quality data were not available for all parameters and all storm periods identified due to some gaps in the data records. However, in total, the analysis was completed on 64 storms for nitrate-N, 41 storms for TP and 60 storms for turbidity at Brixton Deverill, and on 76 storms for turbidity at Prior's Farm over the two year monitoring period. For each storm, the discharge was plotted against each water quality parameter to analyse for the presence and characteristics of hysteresis during each event. A series of metrics were then calculated to describe the storm event and the resultant hysteresis loop, including shape and area. Full details of all the metrics calculated are detailed below.

2.4.1. Storm characteristic metrics

Each storm was described by a number of variables which were hypothesised as potential controls on the form of the measured water quality response. The minimum, maximum and range of discharge and the chemical parameters were calculated, along with event duration (days), and the average discharge in the 24 h preceding the storm. A daily antecedent precipitation index was also calculated as a simple assessment of catchment wetness, using the method described by Saxton and Lenz (1967):

$$API_j = K(API_{j-1} + P_{j-1})$$

where j is the time step (days), P is the daily precipitation total (mm) and K is a decay coefficient. The value of K is primarily controlled by evapotranspiration and, as a result, it was assumed that the value was similar between the two field sites. Saxton and Lenz (1967) suggested a range of K values (0.86–0.98) depending on season and other site-specific conditions. Due to a lack of robust evidence for deriving the value for the specific evapotranspiration and soil characteristics of the Hampshire Avon study catchments, the range of expected values outlined by Saxton and Lenz (1967) was used in all of the analyses. In addition to API, the rainfall total for the 24 h period preceding the start of the storm event (mm) and the total event rainfall (mm) were also calculated.

2.4.2. Storm response hysteresis metrics

The storm hysteresis loops were described by their size and shape following the methods outlined by Lloyd et al. (2015a). The area inside each loop was calculated for the raw data and for normalised data where 0 is the minimum and 1 is the maximum discharge/water quality value for each individual storm event. The loop shape (in terms of its fatness) and direction were determined with the use of a hysteresis index (HI). There are a number of indices which have been proposed to describe the shape and direction of hysteresis loops (e.g. Butturini et al., 2008; Langlois et al., 2005; Lawler et al., 2006), however, a new method is used here which improves the methodology (Lloyd et al., 2015a). This uses the range of chemical data values between the rising and falling limb at multiple percentiles of discharge rather than, for example, the ratio method which was initially proposed by Lawler et al. (2006) as further analysis has shown that skew can be introduced into the results using the latter method. A full discussion of the impact of the modified methodology on index results can be found in Lloyd et al. (2015a). The new index is calculated using storms which have first been normalised using the following equations:

$$Normalised\ Q_i = \frac{Q_i - Q_{min}}{Q_{max} - Q_{min}}$$

$$Normalised\ C_i = \frac{C_i - C_{min}}{C_{max} - C_{min}}$$

where: Q_i/C_i is the discharge/turbidity at timestep i, Q_{min}/C_{min} is the minimum storm parameter value and Q_{max}/C_{max} is the maximum storm parameter value. The index is then calculated as follows:

$$HI_{Q_i} = C_{RL\_Qi} - C_{FL\_Qi}$$

where: HI_{Qi} is the index at percentile i of discharge (Q), C_{RL_Qi} is the chemical value on the rising limb at percentile i of Q and C_{FL_Qi} is the chemical value at the equivalent point in discharge on the falling limb. The percentiles of discharge (Q_i) are defined by:

$$Q_i = k(Q_{max} - Q_{min}) + Q_{max}$$

where Q_{max} is the peak discharge, Q_{min} is the discharge at the start of the event and k is the point along the loop where the calculation is being made; in this case the index was calculated at every 5% of discharge, therefore $k = 0.05, 0.1 \ldots 0.95$. By taking this approach, the index better represents the changing dynamics during a storm event yet still provides one value which can be compared easily between storms. The simple index is easy to interpret; it produces a result between −1 and 1, where the larger the number the 'fatter' the loop and the sign of the index illustrates the direction of the loop (+ = clockwise and − = anti-clockwise).

In addition, nitrate-N and TP loads for each storm were calculated using the paired 30 min resolution discharge and nutrient observations.

Relationships between individual calculated storm characteristic variables and the storm response hysteresis metrics were tested using correlation analysis. The influence of variables in combination on the hysteresis metrics was tested using multiple regression analysis. The examination of correlation plots between the variables provided no clear evidence of non-linearities, therefore multiple linear regression was deemed an appropriate technique. Care was taken to ensure that the normality assumptions were met and any variables which were strongly correlated were omitted from the analysis to satisfy the multicollinearity assumption.

3. Results

3.1. Data uncertainty

The time series of discharge, nitrate-N, TP and turbidity for Brixton Deverill for the two year monitoring period are shown in Fig. 2. The discharge at Brixton Deverill is primarily groundwater driven resulting in a hydrograph with a slow changing baseflow component with more flashy responses during storm events, potentially driven by near-surface and overland flow. The uncertainties in the discharge measurements were heteroscedastic and ranged from ±2.2–9.1% depending on the stage height. The nitrate-N time series tended to mirror the river flow pattern, with peaks in discharge corresponding with dilution of nitrate-N as the surface water input acted to dilute the relatively nitrate-rich groundwater in the stream. The other notable feature in the nitrate-N data collected at Brixton Deverill is the decrease in concentration which occurred in June 2013, corresponding to the switching on of stream support by the local water company during the dry summer period of that year. The decrease in concentration of nitrate-N in the groundwater over this period is also supported by the fortnightly grab samples collected as part of the Hampshire Avon DTC from the borehole at Kingston Deverill 2.7 km upstream from Brixton Deverill, where nitrate-N concentrations decreased from 7.4 mg L^{-1} to 6.4 mg L^{-1} between July 2013 and November 2013 (unpublished data). Fig. 2b also shows the uncertainty bounds around the nitrate-N data measured using the Nitratax sensor, with the error ranging from 0.35 and 0.41 mg L^{-1} (±5–33%). Fig. 2c and d shows that in contrast to nitrate-N, TP and turbidity both show increases in their concentrations during storm events which confirms behaviours reported in earlier research, cited above. The close agreement between TP and turbidity (as a surrogate for sediment transport) responses has been noted in many studies (see for examples: Evans et al., 2003; Evans et al., 2004; Kronvang et al., 1997; Ramos et al., 2015). The uncertainties in the TP sensor data were quantified as being between 0.098 and 0.11 mg L^{-1} (±7–204%). The uncertainty estimate for the turbidity data at Brixton Deverill was ±0.9 NTU (0.2–180%).

Fig. 3 shows the discharge and turbidity time series for the Sem at Prior's Farm. Compared with the chalk landscape of the Wylye, because the headwaters of the Sem are underlain with clay, the hydrograph displays flashy storm responses to rainfall events and a stable but low baseflow between storms. The uncertainties associated with the discharge measurements in the clay were also higher than in the chalk catchment, at ±7.8–25.5%. This is likely to be due to the higher sediment load transported in the water column in this clay catchment, which can reduce velocity sensor performance (Nord et al., 2014), as well as the low velocities experienced at the field site. The turbidity time series shows rapid response and recovery due to discharge events similar to those observed in the Wylye. The uncertainties associated with the turbidity measurements at Prior's Farm were quantified as ±1.5 NTU (0.1–1500%). The discharge and water quality parameter time series and their associated uncertainties were then used to examine hysteresis in the systems on a storm-by-storm basis.

3.2. Storm nutrient behaviour

For each storm the loop area, hysteresis index and storm load (nitrate-N and TP only) were calculated. Given poor ratings between turbidity and filtered suspended sediment concentrations, storm period

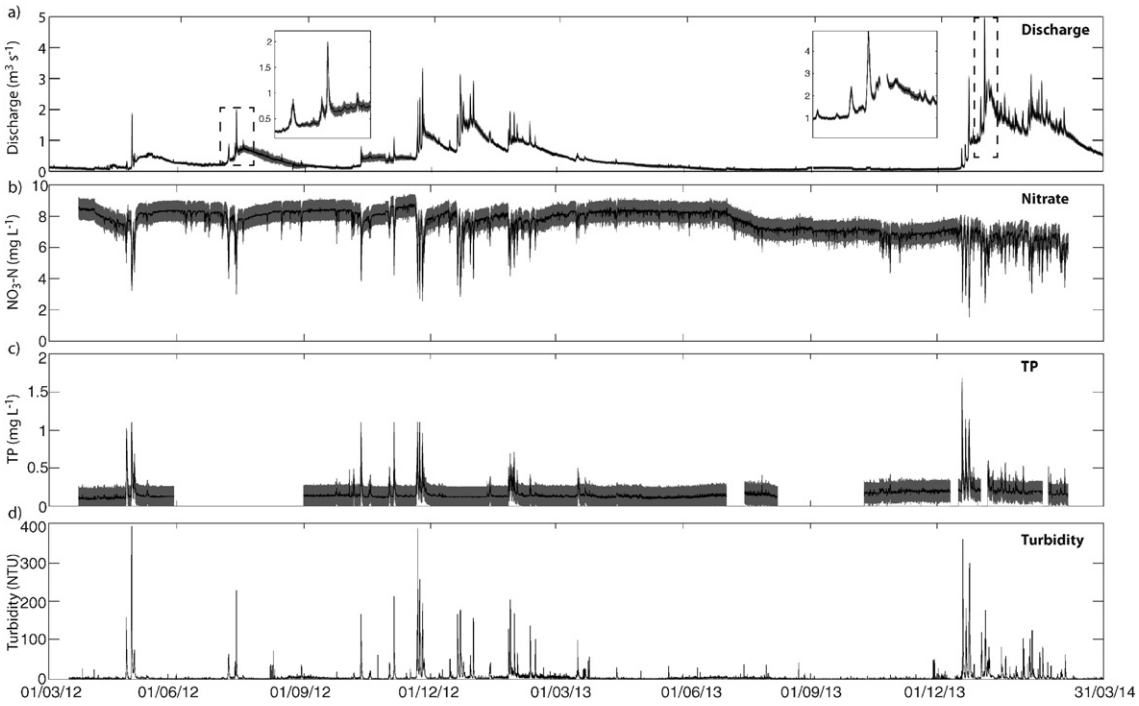

Fig. 2. Plots showing a two year time series of a) discharge, b) nitrate-N, c) TP and d) turbidity for the River Wylye at Brixton Deverill. Grey areas represent data uncertainty (10th–90th percentiles). Dashed boxes highlight expanded sections which are inset.

suspended sediment load data could not be calculated. A range of storm characteristic variables were then used to explain the behaviour of each of the measured water quality parameters. The results are summarised below.

3.2.1. Nitrate hysteretic behaviour

A total of 64 storms were analysed for nitrate-N response, including 3 anti-clockwise events and 61 clockwise events. None of the storms showed figure-of-eight behaviour, and all of the events the hysteresis loops plotted from the top-left to bottom right due to the dilution of nitrate-N on the rising limb of each storm event. Example normalised nitrate-N loops for Brixton Deverill are presented in Fig. 4a. Fig. 5 shows how the loop area, hysteresis index (HI) and storm event load vary through time. The average HI value varied between −0.09 and 0.47, with an average of 0.24 but with non-stationary variations in uncertainty limits. The largest uncertainties tended to be observed for small storms where discharge remained around or below 1 $m^3\ s^{-1}$ and discharge uncertainties were high, this also corresponded to storms where nitrate-N concentrations remained high as there was limited dilution during the event, resulting in higher uncertainties in the nitrate-N concentrations. There were no obvious seasonal trends within the HI data for nitrate-N (see Fig. 5a), although the two events with the largest negative value for the HI both occurred shortly after prolonged dry periods. Analyses showed that the nitrate HI value had a moderate positive correlation (correlation coefficient < 0.4, $p \leq 0.05$) with the range of nitrate-N concentrations during the storm with a negative correlation with the minimum nitrate-N concentrations during the storm. The HI was also correlated to a lesser extent (correlation coefficient < 0.3, $p \leq 0.05$) with the range in discharge and the duration of the storm event. Details are presented in Table 2. Examining the influence of combinations of variables using multiple regression showed that the range in discharge during the storm and the minimum nitrate-N concentration combined were able to explain 47% of the variance in the HI ($p = \leq 0.001$).

Storms at Brixton Deverill showed an average nitrate-N hysteretic loop area of 0.28, with values ranging from 0.01 to 1.22 over the two year period (Fig. 5b). The uncertainty analysis showed that the largest uncertainties were observed for the largest discharge events. As with

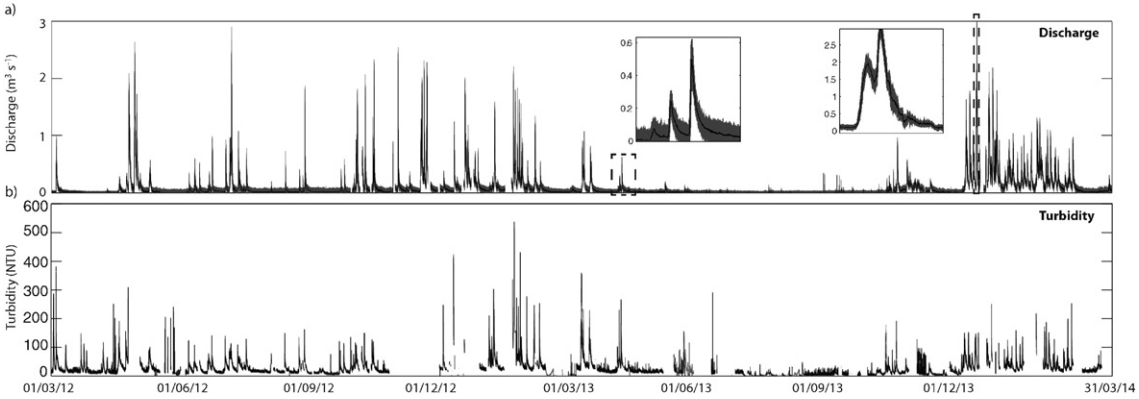

Fig. 3. Plots showing a two year time series of a) discharge and b) turbidity for the River Sem at Prior's Farm. Grey areas represent data uncertainty (10th–90th percentiles). Dashed boxes highlight expanded sections which are inset.

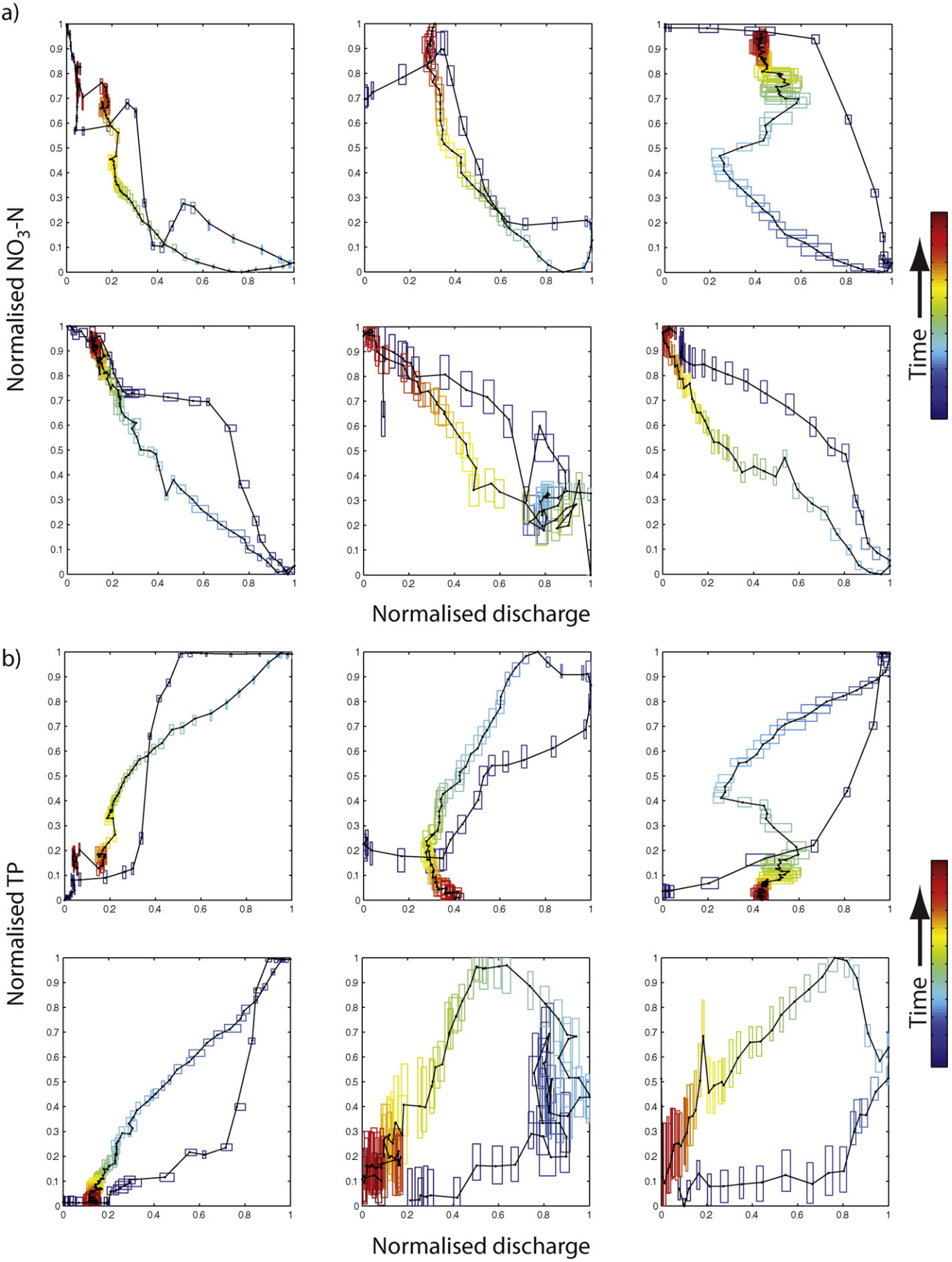
a)
Normalised NO_3-N
Normalised discharge
Time
b)
Normalised TP
Normalised discharge
Time

the HI results there were no clear seasonal trends in loop area, although the largest loop areas tended to be associated with the highest discharge peaks, especially after drier antecedent periods. This is supported by the correlation analysis which showed that loop area was positively correlated with the range of discharge during the event (coefficient 0.85, $p \leq 0.05$). Loop area was also positively correlated with the range of nitrate-N concentrations during the storm along with the minimum nitrate-N concentration (negatively). The loop area was also shown to be related to the storm duration and the maximum discharge value during the storm. Multiple regression analysis revealed that 49% of the variance in loop area ($p \leq 0.001$) could be explained with a combination of storm duration, the maximum discharge during the storm and the time elapsed since the previous storm event.

The storm loads at Brixton Deverill ranged from 57 kg N to 1911 kg N, with an average of 80 kg N transported per storm. In general, the storm nitrate-N loads mirrored the discharge behaviour, the largest nitrate loads were associated with the biggest discharge events (Fig. 5c). Like the loop area the largest uncertainties in the storm load were also observed for the larger discharge events. Over the monitoring period this meant that the largest nitrate loads were observed during the winter and spring. Correlation analysis (Table 2) showed that the total event nitrate load was strongly and positively (correlation coefficient > 0.6, $p \leq 0.05$) related to the maximum storm discharge, minimum storm discharge and the mean discharge 24 h before the start of the event. Multiple regression analysis showed that maximum discharge during each storm along with storm duration and time since the previous storm could explain 68% of the variance ($p \leq 0.001$) in the nitrate load data.

The correlations between the HI, the storm load and loop area were also tested. There was no significant correlation between the HI and the loop area, and there was a weak correlation between HI and the storm load (mean coefficient −0.3), however only 32% of repeat datasets were significant ($p \leq 0.05$). The analysis also showed that there was no significant relationship between the loop area and the storm load.

3.2.2. Total phosphorus hysteretic behaviour

Data were available to analyse 41 storms for total phosphorus transport in the Wylye at Brixton Deverill, of which 35 exhibited anti-clockwise behaviour and 6 storms clockwise behaviour. Examples of TP hysteresis loops at Brixton Deverill (directly comparable with the storms presented in Fig. 4a for nitrate-N) can be seen in Fig. 4b. While the hysteretic behaviour was generally more complex compared with nitrate-N, only 6 of the storms exhibited figure-of-eight behaviours and all of the storms resulted in an increase in TP concentrations on the rising limb of the hydrograph. Fig. 6a shows the results of the H index calculations for each storm. The minimum value was −0.65 and the maximum 0.21, with an average of −0.24. The uncertainty analysis showed that the widest uncertainty bounds around the HI values were for small storms where the percentage discharge uncertainty was high. The data show that as well as more storms displaying anti-clockwise behaviour, the strength of the hysteresis was also stronger. The time series also showed that clockwise hysteresis generally occurred during the first sizable event after a dry period. Two of the cases of clockwise behaviour were also figure-of-eight where for more than half of the storm the hysteresis was clockwise. The other cases of figure-of–eight behaviour all followed larger clockwise storms, reflecting a changing relationship between discharge and TP transport during each event. The causal mechanisms for explaining the H index behaviour was much more difficult to ascertain for the TP behaviour. None of the tested variables showed significant correlations with H index (see Table 3), however, the multiple regression modelling showed that the mean discharge 24 h before the event (which as correlated with the minimum discharge during the storm) could explain 58% of the variance in the H index data ($p \leq 0.001$), suggesting that the timing of the storm relative to other events was one of the main drivers for the hysteretic behaviour. This may reflect the exhaustion of proximal sources and in-channel P stores in prior events, with activation of sources more distant from the stream in combination with the steady discharge of P from proximal point sources in such events.

Fig. 6b shows a time series of the TP loop area measured for each of the storms. The minimum loop area was 0.002 and the maximum 0.35, with an average of 0.05. The largest uncertainty bounds were observed for large storms where both discharge and TP uncertainty played a role. In general, the largest loop areas tended to be associated with the largest discharge events or after drier periods, and therefore coincided with the clockwise and the figure-of-eight hysteretic patterns. The TP loop areas were significantly correlated with range of discharge during the event, the maximum discharge (although these are correlated with each other) and the range of TP values during each event (coefficients 0.79, 0.73 and 0.77 respectively, $p \leq 0.05$), suggesting that the relative magnitude of the storm is an important control alongside the timing of the event. These findings are also supported by the multiple regression results which showed that a combination of the range of discharge during the event and the time since the last storm occurred could explain 68% of the variance in the TP loop area data ($p \leq 0.001$). The TP load during each storm was also calculated and, the results can be seen in Fig. 6c. The analysis showed that the minimum TP event load was 14 kg and the maximum was an order of magnitude higher at 127 kg, with an average TP event load of 33 kg. The largest uncertainty bounds were observed for large storms or for storms occurring after drier periods, i.e. where the TP concentrations were high. As with the nitrate-N data, the time series shows that the magnitude of the TP load mirrored the discharge, with the largest TP loads recorded during the highest magnitude discharge events. The correlation analysis showed that the most important controls on the TP load were the range of discharge during the event (0.84), maximum discharge (0.71), maximum TP (0.56) and the range of TP concentrations (0.51) (all $p \leq 0.05$). The multiple regression analysis showed that a combination of the storm duration, the range in discharge and the minimum TP concentration could account for 95% of the variance in the TP load data ($p \leq 0.001$).

The examination of the correlations between the storm hysteresis metrics measured showed that there was a weak positive relationship (coefficient = 0.4) between the HI value and the storm load, however only 58% of the distribution of values were statistically significant ($p \leq 0.05$). Likewise there was no significant relationship between the HI value and the loop area. However, there was a significant positive relationship between the loop area and the storm load (coefficient = 0.59, $p \leq 0.05$ for 100% of the distribution).

3.2.3. Turbidity hysteretic behaviour

A total of 60 storms were tested for hysteresis behaviour of turbidity for the Wylye at Brixton Deverill, for examples see Fig. 7a. The analysis showed that 37 of the storms demonstrated anti-clockwise hysteresis and 23 were clockwise. The turbidity data showed the most complex hysteretic behaviour when compared with the nutrient chemistry, with 25 of the storms exhibiting figure-of-eight behaviour. The time series of H index values is shown in Fig. 8a, and shows that the clockwise hysteresis was associated with the largest storm events or smaller storms which occur after periods of lower discharge. The minimum value for the H index was −0.65 and the maximum 0.21, with an average of −0.24, showing that the although 38% of the storms showed clockwise hysteresis, the strength of the hysteresis was weak compared with the anti-clockwise behaviour which produced much wider loops. The most uncertainty again was associated with the smaller storms where the percentage uncertainty was greatest for both discharge and turbidity values. This also meant that over a series of storms the

Fig. 4. Plots showing example normalised hysteresis loops for a) nitrate-N and b) TP for storms at Brixton Deverill. The boxes represent the 10th–90th percentiles of the uncertainty associated with the discharge and the nutrient data.

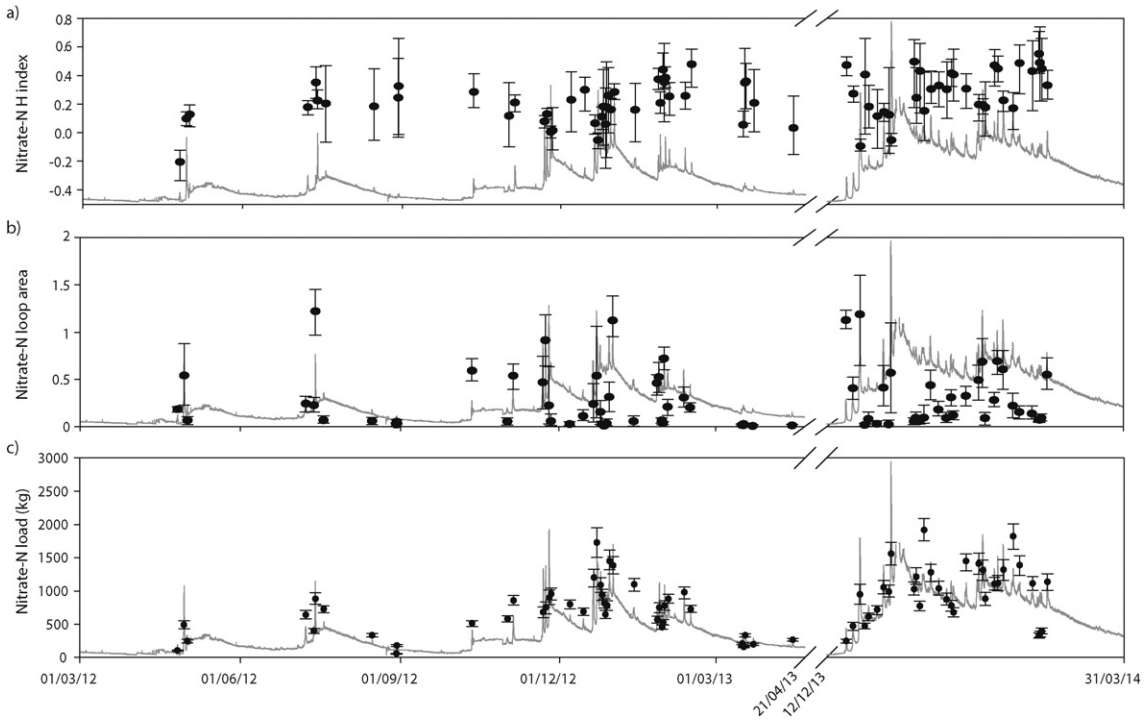

Fig. 5. Plots showing time series of a) H index, b) loop area, and c) loop load for nitrate-N at Brixton Deverill. Error bars represent the 10th–90th percentile range of the values gained from the 100 resampled storms.

uncertainty range increased due to reducing turbidity values and therefore higher percentage uncertainties. Correlation analysis (Table 4) showed that both the turbidity and discharge characteristics during the storm were equally important, displaying similar correlation coefficients (0.51 and 0.48 for range in discharge and turbidity respectively, $p \leq 0.05$). This is supported by the multiple regression analysis which highlighted that the maximum discharge, range in discharge and the maximum turbidity value could be used in combination to explain 74% of the variance in the H index values ($p \leq 0.001$).

The loop area was also calculated for each of the storms and is shown in Fig. 8b. The minimum loop area was calculated as 0.002 and the maximum as 263, with an average value of 20.6. The uncertainty range was generally low for loop area, although unlike the HI values, discharge uncertainty appeared to dominate and therefore the largest ranges were seen for the storms with the highest discharge. The majority of the loops showed small areas (below 50) with the higher values occurring in eight of the storms, all of which corresponded with the largest clockwise hysteresis and occurred when there was an abrupt change in the discharge and few preceding storm events. The loop area showed strong correlations (coefficient > 0.7) with both the range and maximum turbidity values, but only with the range in discharge values, suggesting that the relative change in discharge was more important than the absolute magnitude of the storm. There were also moderate positive correlations with maximum discharge and the duration of the storm (coefficients of 0.48 and 0.46 respectively). Multiple regression analysis showed that a combination of maximum discharge and maximum turbidity during the storm event could explain 64% of the variance in loop area. As with the other parameters measured at Brixton Deverill there was no significant correlation between HI and loop area.

Turbidity data were also analysed for the surface water dominated clay catchment of the Sem at Prior's Farm, allowing a direct comparison with the data generated for the groundwater dominated chalk catchment of the Wylye at Brixton Deverill. Examples of the hysteresis in turbidity at Prior's Farm can be seen in Fig. 7b. A total of 76 storms were investigated over the two year monitoring period and in stark contrast to the chalk site, 69 of the storms exhibited clockwise hysteretic behaviour, with only 7 anti-clockwise, suggesting that the timing of in-channel sediment transport between the two systems was different. There were also fewer storms showing figure-of-eight behaviour compared with the chalk system. The H index data for turbidity at Prior's

Table 2
Results of correlation analysis for each of the 10,000 resampled storm nitrate data at Brixton Deverill, showing the maximum, minimum and modal correlation coefficients and the number of resampled data sets where the p-value was significant (<0.05).

	H index				Loop area				Storm load			
	Min	Max	Mode	Significant	Min	Max	Mode	Significant	Min	Max	Mode	Significant
Duration	0.23	0.48	0.3	9600	0.43	0.64	0.59	10,000	0.36	0.45	0.36	10,000
Max Q	−0.27	0.26	0.25	311	0.41	0.63	0.53	10,000	0.71	0.80	0.77	10,000
Min Q	−0.32	0.23	0.024	3139				0	0.61	0.7	0.67	10,000
Range Q	0.23	0.52	0.387	9927	0.74	0.91	0.85	10,000	0.38	0.54	0.47	10,000
Max NO_3	−0.34	0.23	−0.1	330	−0.35	−0.23	−0.25	4092	−0.43	−0.23	−0.34	9998
Min NO_3	−0.53	−0.23	−0.42	9998	−0.87	−0.7	−0.78	10,000	−0.45	−0.31	−0.39	10,000
Range NO_3	0.26	0.59	0.44	10,000	0.7	0.87	0.78	10,000	0.23	0.31	0.23	4504
Mean Q 24 h	−0.32	−0.23	−0.27	3501				0	0.57	0.68	0.62	10,000
API				0				0	0.48	0.58	0.52	100
Time last storm				0	0.21	0.36	0.23	8900	−0.24	−0.21	−0.24	4500

Farm showed a maximum index of 0.59 and a minimum of −0.17, with an average of 0.23 (Fig. 8c). This is also different from Brixton Deverill, where the widest hysteresis loops were clockwise in their direction and those storms which showed anti-clockwise behaviour had low values of the index. The uncertainties surrounding the HI values were generally larger compared with those calculated from Brixton Deverill, this is due to increased uncertainties in both the measurement of discharge and turbidity at Prior's Farm. However, similar to Brixton Deverill the highest uncertainties were observed for the smallest storms where the percentage uncertainty was greatest for both discharge and turbidity. Unlike the chalk system there were some significant correlations between the H index values and the explanatory variables (Table 5). The strongest correlations with H index were the maximum turbidity and maximum discharge (coefficients of 0.59 and 0.49 respectively, $p \leq 0.05$). The multiple regression analysis highlighted the range in discharge and the maximum turbidity as controls over the H index. However, no combination of explanatory variables could improve the regression r^2 value above 0.32 ($p \leq 0.001$).

The minimum turbidity loop area was 6.21, larger than that for Brixton Deverill, although the maximum was similar between the two field sites at 265 (Fig. 8d). The average loop areas were also comparable at 20.99. The largest uncertainties again were linked to the largest discharge or turbidity values. Like many of the other variables, the larger loop areas coincided with the highest discharge events and with strong clockwise hysteretic patterns. The strongest correlations between turbidity event load and the explanatory variables were with the maximum and range in both discharge and turbidity (coefficients all >0.8, $p \leq 0.05$). There was also a weak correlation between loop area and the duration of the storm (0.28, $p \leq 0.05$). Despite the lower correlation for the Prior's Farm site compared with the analysis at Brixton Deverill, the duration of the storm was shown to be an important variable in combination with the range in discharge and the maximum turbidity values during the event ($r^2 = 0.77$, $p \leq 0.001$), suggesting that the length of the storm is a significant control on sediment mobilisation and transport in this river. Unlike turbidity at Brixton Deverill, HI and loop area were significantly linked at Prior's Farm, with a correlation coefficient of 0.33 and $p \leq 0.05$ for 100% of the distribution tested.

4. Discussion

4.1. Controls on nitrate-N transport

The transport of nitrate-N during storm events in the River Wylye was shown to be primarily controlled by the interaction between groundwater and surface water inputs to the stream. All of the storm events consistently resulted in dilution of nitrate-N concentrations with the input of rainfall and surface runoff. This type of response has been widely reported for other agricultural watersheds (Bowes et al., 2015; Ferrant et al., 2013). However, this is in contrast to other groundwater dominated systems which have shown a mixture of both dilution and concentration events during periods of high rainfall (Huebsch et al., 2014; Webb and Walling, 1985). The specific response depends on the availability of nitrate from proximal sources accumulated in fertilised agricultural soils, in the near-stream unsaturated zone, or in the hyporheic zone where rapid flushing of nitrate-rich soil and groundwater can occur at the start of the storm. However, it should be noted that previous published data from a similar location on the River Wylye during 2010–2011 showed that there was, in fact, a positive relationship between the daily nitrate-N concentrations and discharge, suggesting that storm events could be producing lagged pulses of nitrate-N into the stream as delayed throughflow arrived in stream from groundwater sources (Yates and Johnes, 2013). The average nitrate-N concentrations at Brixton Deverill reported by Yates and Johnes (2013) was 6.39 mg L^{-1}, with concentrations only reaching 7 mg L^{-1} during winter and spring months, with data reported for a relatively dry water year. These concentrations are generally lower than those observed during 2012–2014, with wetter water years, where concentrations were in the range 7–8 mg L^{-1} during baseflow periods. There is also no longer a strong seasonal change in the nitrate-N concentrations compared with the 2010–2011 period. This is potentially due to the differences in the hydrological regime between the two time periods. The largest discharge during the 2010–2011 period was 0.5 m^3 s^{-1} compared with >2 m^3 s^{-1} during the 2012–2014 period. There was no evidence to suggest that there had been any significant changes in land use or farming practices during the study period to account for these changes,

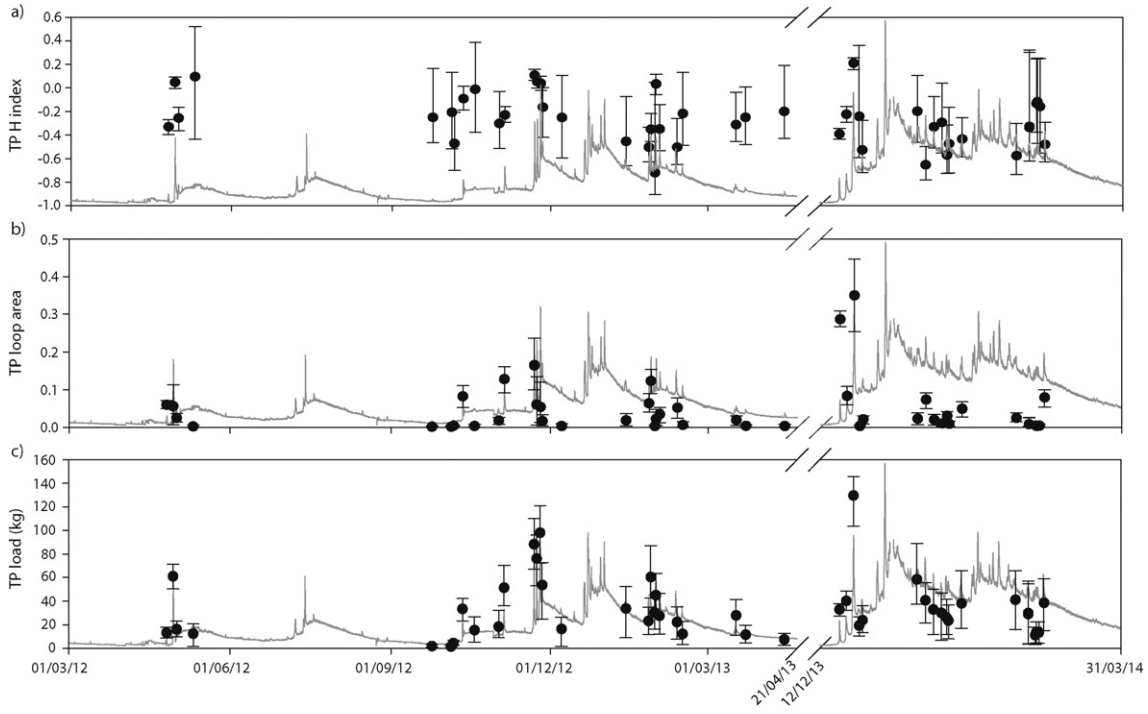

Fig. 6. Plots showing time series of a) H index, b) loop area, and c) loop load for TP at Brixton Deverill. Error bars represent the 10th–90th percentile range of the values gained from the 100 resampled storms.

Table 3
Results of correlation analysis for each of the 10,000 resampled storm total phosphorus data at Brixton Deverill, showing the maximum, minimum and modal correlation coefficients and the number of resampled data sets where the p-value was significant (<0.05).

	H index				Loop area				Storm load			
	Min	Max	Mode	Significant	Min	Max	Mode	Significant	Min	Max	Mode	Significant
Duration	−0.59	−0.30	−0.38	2400	0.30	0.55	0.38	9800	0.29	0.37	0.29	1000
Max Q	0.30	0.40	0.30	706	0.3	0.54	0.40	10,000	0.51	0.82	0.71	10,000
Min Q	0.30	0.40	0.32	976				0				0
Range Q	−0.46	−0.30	−0.31	605	0.64	0.90	0.785	10,000	0.72	0.93	0.84	10,000
Max TP	−0.53	−0.30	0.31	2017	0.49	0.87	0.73	10,000	0.38	0.66	0.56	10,000
Min TP	0.30	0.64	0.31	1182	0.29	0.45	0.3	419	0.29	0.58	0.42	9043
Range TP	−0.53	−0.30	−0.33	3869	0.57	0.83	0.77	10,000	0.36	0.62	0.51	10,000
Mean Q 24 h	0.30	0.40	0.32	874				0				0
API	0.31	0.46	0.39	13				0				0
Time last storm				0	0.30	0.55	0.3	9700				0

supporting the theory that the changes were driven be hydro-meteorological conditions. Marked inter-annual differences in hydrochemical flux behaviours and both nutrient and sediment load transport due to changes in the hydrological regime have been reported previously in the literature (e.g. Borah et al., 2003; Davis et al., 2014; Heathwaite and Johnes, 1996; Prior and Johnes, 2002). For example, Davis et al. (2014) compared nitrate fluxes in an agricultural catchment between wet and dry years and showed that antecedent conditions were important and determined the dominant flow pathways operating and therefore the storm nitrate concentrations.

In this more detailed analysis of storm driven nitrate-N flux in the Wylye chalk catchment, both the H index and the loop area were shown to be influenced by the maximum discharge during the events and the H index also by the minimum discharge. This indicates that the range of discharge during the storm acts to widen the hysteresis loop, due to a change in the lag between the peak in discharge and the minimum nitrate-N concentration. Unlike any of the other chemical parameters studied in this paper for Brixton Deverill, nitrate-N hysteresis was also linked with the duration of the storm. This illustrates that the transport of nitrate-N in this case is relatively straightforward, suggesting that the longer the storm, the more nitrate-N is transported, as nitrate rich soil and groundwater is flushed to the stream along throughflow and groundwater flow pathways present in this permeable catchment. In addition, there was a link between nitrate-N loop area, storm nitrate-N load and the time since the last storm occurred, shown by the multiple regression analysis. This showed that narrower loops were produced when storms occurred temporally close together, probably because the concentrations had not fully recovered to their baseline values before the onset of the next event, and available near-stream proximal sources had been flushed during the previous storm.

4.2. Controls on TP transport

In comparison with nitrate-N, TP transport in the Wylye at Brixton Deverill was shown to be much more complex. The storm events consistently produced pulses of TP to the stream in association with increasing discharge, highlighting that the main source of the TP was probably from surface or near surface quickflow pathways, rather than from groundwater flow through the hyporheic zone. This is also supported by data collected from a nearby groundwater borehole at Kingston Deverill which showed a mean annual TP concentration of 0.19 mg L^{-1}, which is similar to the average baseline concentrations in the River Wylye under baseflow conditions. The mean storm maximum concentration observed in this study was 0.4 mg L^{-1}. The correlation analysis showed no clear links between any of the explanatory variables and the H index. Only the minimum discharge during the event, which was correlated with the mean discharge 24 h before the start of the event was highlighted as important through the multiple regression analysis. This suggests that antecedent conditions are important in controlling TP flux during storm events, though stream discharge was more important than antecedent rainfall patterns (assessed using API). This is in direct contrast to data collected for a groundwater influenced stream in Cumbria, where similar analysis showed that the magnitude of hysteresis was primarily controlled by antecedent rainfall conditions (Bieroza and Heathwaite, 2015). A similar finding was previously reported for the Enborne, UK, which is a comparable chalk stream to the Wylye, where a higher TP flux in storm events occurred when dry antecedent conditions were observed in the catchment. This was attributed to the re-suspension of P-rich fine-grained bed sediment that had accumulated within the channel during summer low flows periods (Evans and Johnes, 2004). The authors also noted that in the Enborne catchment, events characterised by dry antecedent conditions caused higher P transport fluxes than events with higher magnitude flows, a finding recently reported for ephemeral streams in southern Portugal in a recent paper by Ramos et al. (2015). The capacity of channel fine-grained bed sediment to constitute an important store of P liable to remobilisation during storm events has been noted by previous work (e.g. Ballantine et al., 2006; Ballantine et al., 2009; Collins et al., 2005; Davide et al., 2003; House and Denison, 1997; Jarvie et al., 2005; Walling et al., 2003). In the Wylye, the TP loop area was strongly related to discharge characteristics during the storm and the time since the last storm. Bieroza and Heathwaite (2015) showed that the direction of the hysteresis loop was controlled by seasonal variations in flow or changes in temperature controlling nutrient cycling in-stream. Data from Brixton Deverill showed that the hysteresis was more strongly controlled by shorter-term changes in discharge. This effect can be examined by looking in more detail at a series of storms and observing how the hysteresis patterns vary. Fig. 9 shows a series of 4 storms which occurred during November 2012 after a period of approximately two weeks with no rainfall or storm discharge events. The first of the storms exhibited clockwise hysteresis behaviour (H index = 0.11), illustrating a relatively rapid flushing of available TP potentially due to the remobilisation of deposited fine-grained bed sediments during the lower flow period (Ballantine et al., 2009; Dorioz et al., 1998; Evans and Johnes, 2004). The second and third storms in the succession show figure-of-eight behaviours, where the first section of the storm shows anti-clockwise behaviour, before switching to clockwise behaviour later in the event. This causes a decrease in the H index value to 0.04, then 0.03 showing that there is an increasing lag between the peak in discharge and the peak in TP during the storm. This is indicative of a longer transit time between the source of TP and the arrival in-stream. This is supported by the fourth storm in the series, which has switched to anti-clockwise behaviour for the whole storm (H index = −0.2), suggesting a longer transit time again for the TP pulse to reach the monitoring location. This pattern can be observed during other similar periods of discharge events following periods of lower flow and has also been reported elsewhere (Bowes et al., 2005). It is likely that the hysteretic affects are mainly driven by the relative connectivity of P sources in the catchment to the stream system, with delivery primarily controlled by the transport of P-rich sediment from land to

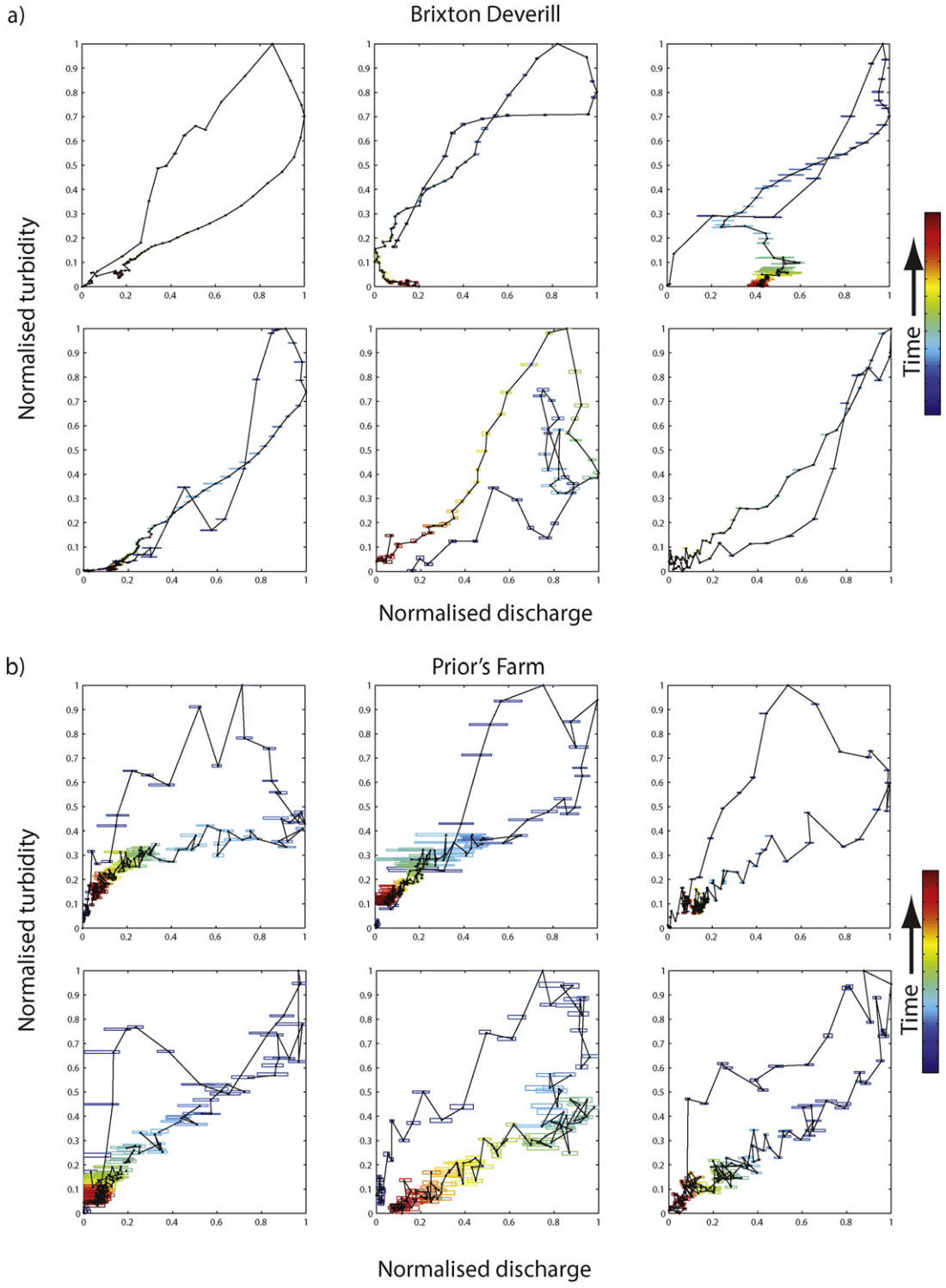

Fig. 7. Plots showing example normalised hysteresis loops for turbidity at a) Brixton Deverill and b) Prior's Farm. The boxes represent the 10th–90th percentile range of the uncertainty associated with the discharge and turbidity data.

water. Daily lab data from Brixton Deverill show that particulate P makes up approximately 20% of the TP signal (the rest being 30% soluble unreactive P and 50% phosphate-P), but that over 80% of P transport at peak flow in storm events is in the form of particulate P. This reflects the activation of P-rich fine-grained sediment transport via quickflow pathways including erosion of fertilised arable soils and subsequent delivery of mobilised P-enriched sediment along tramlines and via field drains, and rapid flow from agricultural yards, along roads and unmetalled agricultural tracks linking land to stream in these landscapes. The capacity of runoff along road networks to mobilise particulate P from roadside verges damaged by passing vehicles and by livestock trampling (e.g. due to daily movements between fields and milking parlours) is also a contributing factor here (cf. Collins et al., 2010a).

This storm pattern is also seen in the turbidity data (see below), supporting the notion that it is the particulate P fraction causing the change in the hysteretic behaviour. In a similar study on the River Enborne, UK, a clay river with chalk headwaters, Bowes et al. (2015)

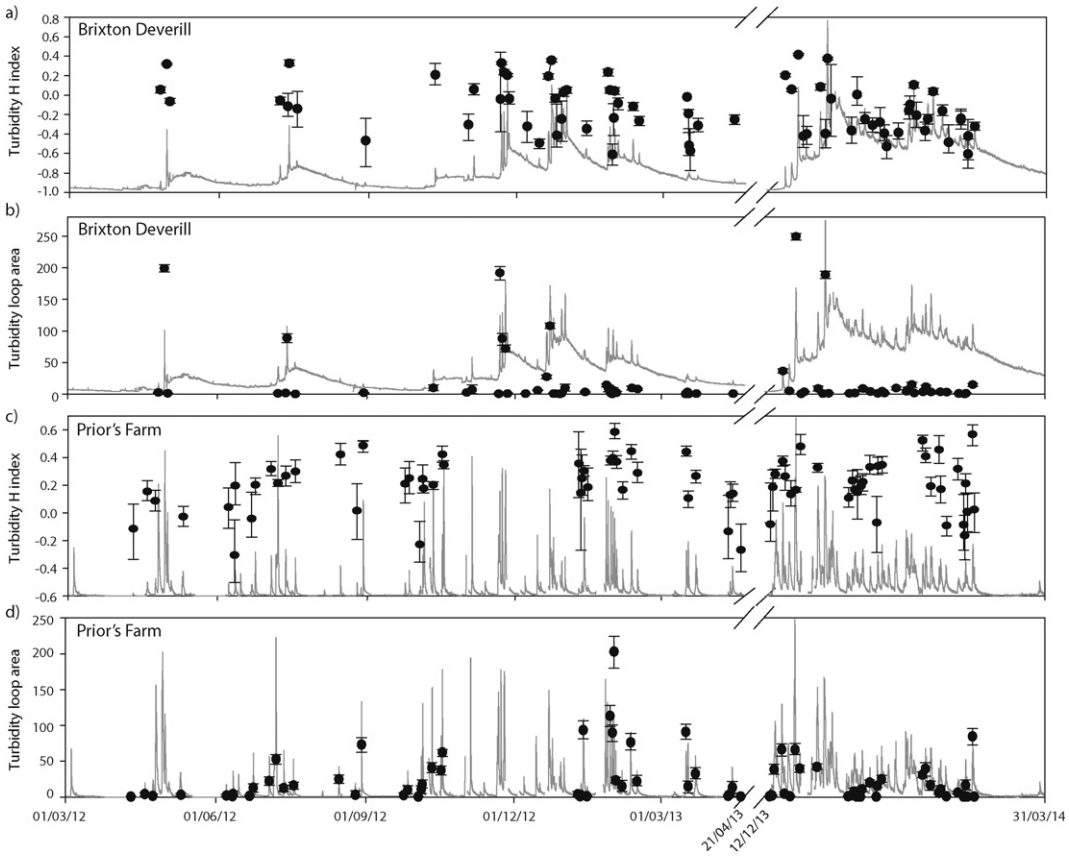

Fig. 8. Plots showing time series of a), c) H index, b), d) loop area for turbidity at Brixton Deverill and Prior's Farm. Error bars represent the 10th–90th percentile range of the values gained from the 100 resampled storms.

observed that during higher discharge conditions the majority of the total reactive P (TRP) load was probably derived from within channel remobilisation of bed sediments. Bowes et al. (2015) state that this is likely to be originally derived from outputs from sewage treatment works, though this contradicts earlier findings by Evans et al. for the same river in an earlier high resolution analysis of phosphorus and sediment transfer dynamics from catchment phosphorus and sediment sources through the water column, and bed sediments of the Enborne (Evans and Johnes, 2004; Evans et al., 2004). In the River Wylye, it is likely that the TP rich material is derived from a combination of erosion of P rich soils from surrounding intensive mixed arable land or from P sorbed to stream-bed sediments, originating from seepage from septic tanks, of which there are a significant number in close proximity to the stream reach upstream from Brixton Deverill. Previous work in permeable catchments similar to the River Wylye by Evans et al. (2003); Collins and Walling (2007a) and Collins and Walling (2007b) has underscored the propensity for fine-grained sediment delivered to the river channel from a variety of sources to undergo channel bed storage during its transit through the channel network. Such bed material undergoes storage and remobilisation in tandem with patterns of runoff and channel discharge, providing an important mechanism for the storage, remobilisation and downstream transport of sediment-associated nutrient fractions such as phosphorus from both point and diffuse catchment sources.

4.3. Controls on sediment transport

Using turbidity as a surrogate for sediment it was possible to infer the potential controls on sediment transport in both a chalk dominated environment as well as a surface water-dominated clay system. Both catchments exhibited peaks in turbidity during storm events in every case, but the timing and characteristics of the hysteresis differed

Table 4
Results of correlation analysis for each of the 10,000 resampled storm turbidity data at Brixton Deverill, showing the maximum, minimum and modal correlation coefficients and the number of resampled data sets where the p-value was significant (<0.05).

	H index				Loop area			
	Min	Max	Mode	Significant	Min	Max	Mode	Significant
Duration	0.24	0.27	0.24	500	0.39	0.56	0.46	10,000
Max Q	0.24	0.32	0.25	7379	0.41	0.54	0.48	10,000
Min Q	−0.21							0
Range Q	0.42	0.55	0.51	9100	0.62	0.85	0.79	10,000
Max turbidity	0.42	0.57	0.50	9100	0.71	0.88	0.82	10,000
Min turbidity	0.34	0.50	0.43	9100	0.23	0.24	0.23	21
Range turbidity	0.40	0.55	0.48	9100	0.71	0.89	0.83	10,000
Mean Q 24 h	−0.27	−0.24	−0.24	167				0
API				0				0
Time last storm				0	0.26	0.26	0.26	100

Table 5
Results of correlation analysis for each of the 10,000 resampled storm turbidity data at Prior's Farm, showing the maximum, minimum and modal correlation coefficients and the number of resampled data sets where the p-value was significant (<0.05).

	H index				Loop area			
	Min	Max	Mode	Significant	Min	Max	Mode	Significant
Duration				0	0.23	0.36	0.28	10,000
Max Q	0.42	0.61	0.49	10,000	0.79	0.89	0.83	10,000
Min Q	0.22	0.30	0.23	762	0.21	0.38	0.27	8861
Range Q	0.44	0.65	0.55	10,000	0.83	0.91	0.87	10,000
Max turbidity	0.50	0.71	0.59	10,000	0.74	0.83	0.80	10,000
Min turbidity	0.22	0.33	0.24	3489	0.34	0.49	0.42	10,000
Range turbidity	0.50	0.70	0.59	10,000	0.74	0.83	0.81	10,000
Mean Q 24 h	0.22	0.23	0.22	13	0.21	0.33	0.22	3654
API				0				0
Time last storm				0				0

between the chalk and the clay catchments. The chalk catchment showed similar behaviour compared with that described for TP above, where the discharge characteristics played an important role in suspended sediment response. Short-term discharge dynamics affected the direction and strength of the hysteretic behaviour, as can be observed in Fig. 7. For the same four storms described above for TP transport, the HI values for turbidity were 0.33, 0.23, 0.2 and −0.03, where the middle two storms were again figure-of-eight. The following two storms showed stronger anti-clockwise hysteresis, with the H index values decreasing to −0.32, then −0.5 as the next two smaller discharge events affect the catchment. After a period of approximately 4 days of hydrograph recession a larger storm occurs and results again in a strong clockwise hysteresis event. This suggests that the larger event was able to either remobilise fine-grained channel bed sediment (cf. Bogen, 1980; Costa, 1977; Wood, 1977) which had been deposited during the recession period (cf. Gellis, 2013) and/or erode a source of sediment which was very close to the monitoring location. The important contribution of remobilised channel bed sediment to suspended sediment fluxes has been reported for lowland permeable catchments in the UK by a wide range of authors (see for example: Collins and Walling, 2006; Evans et al., 2004; Walling and Amos, 1999). Within the River Wylye landscape, a number of potential sediment sources were noted to be proximal to the monitoring station at Brixton Deverill and which would thereby potentially explain the observed pattern noted above. These proximal sources included arable soils with tramlines providing elevated connectivity between fields and delivery routes such as roads to the channel network (cf. Collins et al., 2013), eroding unmetalled farm tracks (cf. Collins et al., 2010b) and poached channel banks (cf. Collins et al., 2013; Walling et al., 2008). Compared with the other nutrient parameters the correlation analyses showed that the turbidity parameters were important alongside the discharge parameters for predicting hysteresis behaviour. The multiple regression analysis showed that the range in discharge along with the maximum turbidity could be used to predict the magnitude of the H index. The relative change in discharge is important for the potential for sediment transport, as a large change means either an increase in the erosive power of the stream, or the period before was relatively low flow and a supply of sediment was therefore either deposited and will thus be available for re-suspension, or that the availability of sediment in various sources increased due, for example, to the action of subaerial weathering processes during the drier spell. This evidence suggests therefore that the fine-grained suspended sediment transport regime at Brixton Deverill is supply-limited and thereby typical of UK rivers more generally (Walling and Webb, 1987).

The hysteretic behaviour of turbidity on the River Sem, on the clay catchment is, however, different. The vast majority of the storms resulted in clockwise hysteresis, regardless of season or size of storm. As for Brixton Deverill, both the range in discharge and the turbidity characteristics were important, but in addition so was the duration of the storm. This type of behaviour has been reported elsewhere, for example, Jiang et al. (2010) observed during storm events in Japan that suspended sediment always showed clockwise hysteresis patterns, compared with nitrate-N and other dissolved components where the type of hysteretic behaviour depended upon antecedent conditions. The continual clockwise hysteresis even during a series of four or five storms over a period of a week suggest that in this surface water-dominated clay catchment, there was an unlimited supply of fine-grained sediment available for mobilisation and subsequent transport to, and through, the stream during storm events, probably from multiple (surface and subsurface) sources in the catchment. In general, the larger the discharge peak the higher the turbidity, resulting in a larger clockwise hysteresis loop. It appears that the transport regime in the clay can be described as transport-limited, i.e. if there is flow which is able to transport fine-grained sediment, there will be a readily available supply of sediment to be transported; antecedent conditions here are therefore not so important. A number of potential sediment sources were observed during catchment walkover surveys in the River Sem study area, the most important of which concerned kilometres of bare, re-worked channel banks (up to 1.5 m high) following a major stream bank fencing programme jointly funded by the Catchment Sensitive Farming initiative and the farmers. These channel works left the channel margins completely prone and susceptible to erosion and sediment mobilisation and delivery due to the negligible transport distances to the river (cf. Collins and Walling, 2004). Although field walks in the Sem catchment highlighted the bare re-worked channel banks as the most likely explanation of the dominance of clockwise hysteresis in the turbidity records, it is noted that clockwise behaviour has been attributed to alternative processes in previous studies including the exhaustion of either surface (Doty and Carter, 1965) or subsurface (Carling, 1983) sediment sources and reductions in surface soil detachment arising from the cessation of effective precipitation (Novotny, 1980). In the case of the study reported here, however, the channel bank works provided the most likely explanation of the clockwise turbidity loops.

4.4. Uncertainty analysis

The work presented here provides one of the first studies to examine hysteresis analysis within an uncertainty framework. The results highlight the importance of incorporating observational uncertainty estimates in the calculation of the H index. There are a proportion of the values that have uncertainty estimates which span from positive to negative values, representing either clockwise or anti-clockwise hysteresis. The largest uncertainties in the H index values were associated with storms where discharge was low. Due to the normalisation before the calculation of the index the uncertainty represents the percentage uncertainty which is large at low discharges compared with the absolute values. Conversely, the largest uncertainly bounds for the loop area and the storm load were observed during the storms with the highest discharges as the absolute values are used in the calculation. It is therefore important to consider the method used for the calculation of the metrics when interpreting the results. The impact of observational uncertainty on the calculation of annual nutrient loads in catchments has already been discussed in detail in Lloyd et al. (2015b), but results from this study support the conclusion that it is important to consider the uncertainties when calculating nutrient loads whether over a single storm, a whole season or a year. By carrying out uncertainty analysis as part of the analytical framework it is possible to produce results which are more statistically sound and produce robust conclusions.

5. Conclusions

The use of high temporal resolution 15 or 30 min hydrological and hydrochemical data in this paper has allowed a detailed analysis of nutrient and fine-grained sediment transport to streams of contrasting

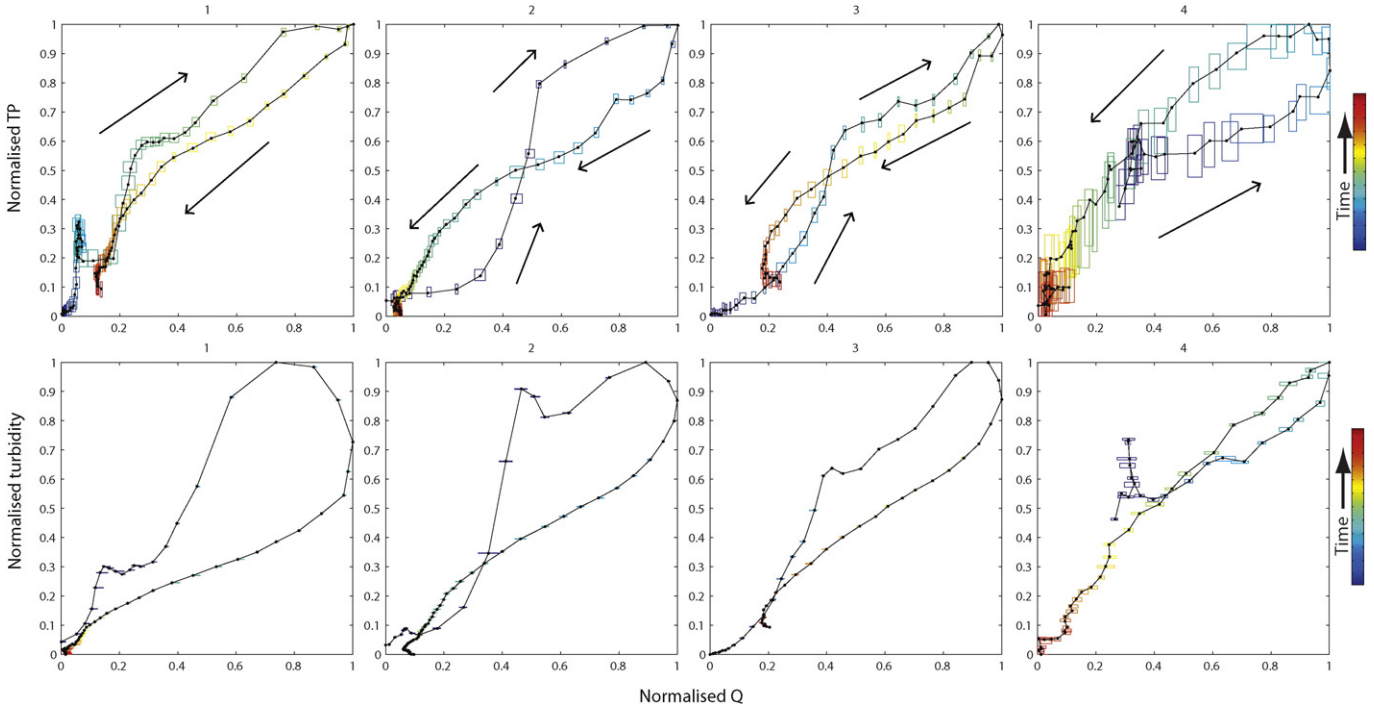

Fig. 9. Plots showing normalised hysteresis loops for a series of four storms for TP and turbidity at Brixton Deverill.

hydrogeological and landscape character under stormflow conditions. The detailed uncertainty analysis incorporated in this work has allowed us, for the first time, to assess the quality of the data available, cascading this uncertainty information through the analysis presented herein. Hysteresis analysis is a valuable tool for assessing storm behaviours and provides a useful way for comparing storms within, and between catchments, as well as comparing different hydrochemical parameter responses to investigate how catchment function varies in time and in relation to catchment character. The analysis presented here confirms that concentration-discharge relationships are extremely complicated, varying between rivers, water years and events, but illustrates clearly how the collection of high resolution data under extreme flow conditions allows a more detailed analysis of these relationships than has hitherto been possible. This in turn provides some novel insights into the catchment processes controlling hydrological response and hydrochemical transport of nutrient loads from land to stream and within the stream itself, both in dissolved and particulate forms. With two years of high resolution information it possible to see difference in the mechanisms which are operating to transport nitrate-N versus TP and fine-grained sediment to the stream in a groundwater dominated system. This study has also clearly shown the different transport regimes operating between a groundwater versus a surface-water dominated catchment. This information, set within an uncertainty framework means that extra confidence can be had that the patterns and relationships are statistically robust. The insights gained from this type of analysis will be invaluable for inferring the likely contributing source areas in catchments, the pathways linking source to stream, and the relative importance of catchment versus instream nutrient and sediment sources to the continued flux of material downstream. It can thus be used to identify the most effective ways to mitigate nutrient pollution and sediment transport in catchments, as well as providing information regarding transport processes and biogeochemical processing within river environments. The analyses presented here are scale dependent in that they are linked to a single sampling station at the outlet of each study catchment. Future work could employ similar monitoring at more locations within a study area to examine potential spatial variations in hysteretic responses and the implications for process understanding and catchment management. Whilst providing a useful basis for inferring catchment responses, hysteresis analysis should be adopted in tandem with other procedures to procure a 'weight-of-evidence' of potential pollutant sources and transport pathways in catchments, and thereby better guide efforts to target sources or interrupt pollutant transport through the implementation of mitigation measures in these catchments.

Acknowledgements

The authors gratefully acknowledge the funding provided by Defra project WQ0211 (the Hampshire Avon Demonstration Test Catchment project) and NERC Grant NE/1002200/1 (The Environmental Virtual Observatory Pilot), and the access to the Brixton Deverill gauging site and flow data provided by Geoff Hardwicke at the Environment Agency.

References

Allen, D.J., et al., 2014. Groundwater conceptual models: implications for evaluating diffuse pollution mitigation measures. Q. J. Eng. Geol. Hydrogeol. 47 (1), 65–80. http://dx.doi.org/10.1144/qjegh2013-043.

Ballantine, D., Walling, D., Collins, A., Leeks, G.L., 2006. Phosphorus storage in fine channel bed sediments. Water Air Soil Pollut: Focus 6 (5–6), 371–380. http://dx.doi.org/10.1007/s11267-006-9029-2.

Ballantine, D.J., Walling, D.E., Collins, A.L., Leeks, G.J.L., 2009. The content and storage of phosphorus in fine-grained channel bed sediment in contrasting lowland agricultural catchments in the UK. Geoderma 151 (3–4), 141–149. http://dx.doi.org/10.1016/j.geoderma.2009.03.021.

Beschta, R.L., 1987. Conceptual models of sediment transport in streams. In: Thorne, C.R., Bathurst, J.C., Hey, R.D. (Eds.), Sediment Transport in Gravel-bed Rivers. Wiley, pp. 387–419.

Bieroza, M.Z., Heathwaite, A.L., 2015. Seasonal variation in phosphorus concentration-discharge hysteresis inferred from high-frequency in situ monitoring. J. Hydrol. 524, 333–347. http://dx.doi.org/10.1016/j.jhydrol.2015.02.036.

Bogen, J., 1980. The hysteresis effect of sediment transport systems. Nor. Geogr. Tidsskr. 34, 45–54.

Borah, D.K., Bera, M., Shaw, S., 2003. Water, sediment, nutrient, and pesticide measurements in an agricultural watershed in Illinois during storm events. Transactions of the Asae 46 (3), 657–674.

Bowes, M.J., House, W.A., Hodgkinson, R.A., 2003. Phosphorus dynamics along a river continuum. Sci. Total Environ. 313 (1–3), 199–212. http://dx.doi.org/10.1016/s0048-9697(03)00260-2.

Bowes, M.J., House, W.A., Hodgkinson, R.A., Leach, D.V., 2005. Phosphorus-discharge hysteresis during storm events along a river catchment: the River Swale, UK. Water Res. 39 (5), 751–762. http://dx.doi.org/10.1016/j.watres.2004.11.027.

Bowes, M.J., et al., 2015. Characterising phosphorus and nitrate inputs to a rural river using high-frequency concentration–flow relationships. Sci. Total Environ. 511, 608–620. http://dx.doi.org/10.1016/j.scitotenv.2014.12.086.
Bowes, M.J., Smith, J.T., Neal, C., 2009. The value of high-resolution nutrient monitoring: a case study of the River Frome, Dorset, UK. J. Hydrol. 378 (1–2), 82–96. http://dx.doi.org/10.1016/j.jhydrol.2009.09.015.
Brater, E.F., King, H.W., 1976. Handbook of hydraulics for the solution of hydraulic engineering problems. McGraw-Hill, New York; London.
Butturini, A., Alvarez, M., Bernal, S., Vazquez, E., Sabater, F., 2008. Diversity and temporal sequences of forms of DOC and NO3-discharge responses in an intermittent stream: predictable or random succession? J. Geophys. Res. Biogeosci. 113 (G3). http://dx.doi.org/10.1029/2008jg000721.
Carey, R.O., Wollheim, W.M., Mulukutla, G.K., Mineau, M.M., 2014. Characterizing storm-event nitrate fluxes in a fifth order suburbanizing watershed using in situ sensors. Environ. Sci. Technol. 48 (14), 7756–7765. http://dx.doi.org/10.1021/es500252j.
Carling, P.A., 1983. Threshold of coarse sediment transport in broad and narrow natural streams. Earth Surf. Process. Landf. 8 (1), 1–18. http://dx.doi.org/10.1002/esp.3290080102.
Chen, N., Wu, J., Hong, H., 2012. Effect of storm events on riverine nitrogen dynamics in a subtropical watershed, southeastern China. Sci. Total Environ. 431, 357–365. http://dx.doi.org/10.1016/j.scitotenv.2012.05.072.
Collins, A.L., Walling, D.E., 2004. Documenting catchment suspended sediment sources: problems, approaches and prospects. Prog. Phys. Geogr. 28 (2), 159–196. http://dx.doi.org/10.1191/0309133304pp409ra.
Collins, A.L., Walling, D.E., 2006. Investigation of the remobilisation of fine sediment stored on the channel bed of lowland permeable catchments in the UK. Sediment dynamics and the hydromorphology of the fluvial system. International Association of Hydrological Sciences, Wallingford, UK, pp. 471–479.
Collins, A.L., Walling, D.E., 2007a. Fine-grained bed sediment storage within the main channel systems of the Frome and Piddle catchments, Dorset, UK. Hydrol. Process. 21 (11), 1448–1459. http://dx.doi.org/10.1002/hyp.6269.
Collins, A.L., Walling, D.E., 2007b. The storage and provenance of fine sediment on the channel bed of two contrasting lowland permeable catchments, UK. River Res. Appl. 23 (4), 429–450. http://dx.doi.org/10.1002/rra.992.
Collins, A.L., Walling, D.E., Leeks, G.J.L., 2005. Storage of Fine-grained Sediment and Associated Contaminants Within the Channels of Lowland Permeable Catchments in the UK.
Collins, A.L., Walling, D.E., Webb, L., King, P., 2010a. Apportioning catchment scale sediment sources using a modified composite fingerprinting technique incorporating property weightings and prior information. Geoderma 155 (3–4), 249–261. http://dx.doi.org/10.1016/j.geoderma.2009.12.008.
Collins, A.L., Zhang, Y., Walling, D.E., Grenfell, S.E., Smith, P., 2010b. Tracing sediment loss from eroding farm tracks using a geochemical fingerprinting procedure combining local and genetic algorithm optimisation. Sci. Total Environ. 408 (22), 5461–5471. http://dx.doi.org/10.1016/j.scitotenv.2010.07.066.
Collins, A.L., Zhang, Y.S., Duethmann, D., Walling, D.E., Black, K.S., 2013. Using a novel tracing-tracking framework to source fine-grained sediment loss to watercourses at sub-catchment scale. Hydrol. Process. 27 (6), 959–974. http://dx.doi.org/10.1002/hyp.9652.
Comber, A., Proctor, C., Anthony, S., 2008. The creation of a National Agricultural Land Use Dataset: combining pycnophylactic interpolation with dasymetric mapping techniques. Trans. GIS 12 (6), 775–791. http://dx.doi.org/10.1111/j.1467-9671.2008.01130.x.
Costa, J.E., 1977. Sediment concentration and duration in stream channels. J. Soil Water Conserv. 32 (4), 168–170.
Coxon, G., Freer, J., Westerberg, I.K., Wagener, T., Woods, R., Smith, P.J., 2015. A novel framework for discharge uncertainty quantification applied to 500 UK gauging stations. Water Resour. Res. 51, 5531–5546. http://dx.doi.org/10.1002/2014WR016532.
Davide, V., et al., 2003. Characterisation of bed sediments and suspension of the river Po (Italy) during normal and high flow conditions. Water Res. 37 (12), 2847–2864. http://dx.doi.org/10.1016/s0043-1354(03)00133-7.
Davis, C.A., et al., 2014. Antecedent moisture controls on stream nitrate flux in an agricultural watershed. J. Environ. Qual. 43 (4), 1494–1503. http://dx.doi.org/10.2134/jeq2013.11.0438.
Dorioz, J.M., Cassell, E.A., Orand, A., Eisenman, K.G., 1998. Phosphorus storage, transport and export dynamics in the Foron river watershed. Hydrol. Process. 12 (2), 285–309. http://dx.doi.org/10.1002/(sici)1099-1085(199802)12:2<285::aid-hyp577>3.0.co;2-h.
Doty, C.W., Carter, C.E., 1965. Rates and particle-size distribution of soil erosion from unit source areas. Trans. Am. Soc. Agric. Eng. 8, 309–311.
Drewry, J.J., Newham, L.T.H., Croke, B.F.W., 2009. Suspended sediment, nitrogen and phosphorus concentrations and exports during storm-events to the Tuross estuary, Australia. J. Environ. Manag. 90 (2), 879–887. http://dx.doi.org/10.1016/j.jenvman.2008.02.004.
European Parliament, E., 2000. Establishing a framework for community action in the field of water policy. In: Parliament, E. (Ed.), Directive EC/2000/60, EU, Brussels.
Evans, D.J., Johnes, P., 2004. Physico-chemical controls on phosphorus cycling in two lowland streams. Part 1 — the water column. Sci. Total Environ. 329 (1–3), 145–163. http://dx.doi.org/10.1016/j.scitotenv.2004.02.016.
Evans, D.J., Johnes, P.J., Lawrence, D.S., 2003. Suspended and bed load sediment transport dynamics in two lowland UK streams — storm integrated monitoring. Erosion and Sediment Transport Measurement in Rivers: Technological and Methodological Advances. 283, pp. 103–110.
Evans, D.J., Johnes, P.J., Lawrence, D.S., 2004. Physico-chemical controls on phosphorus cycling in two lowland streams. Part 2 — The sediment phase. Sci. Total Environ. 329 (1–3), 165–182. http://dx.doi.org/10.1016/j.scitotenv.2004.02.023.
Evensen, G., 2003. The ensemble Kalman filter: theoretical formulation and practical implementation. Ocean Dyn. 53 (4), 343–367. http://dx.doi.org/10.1007/s10236-003-0036-9.
Ferrant, S., et al., 2013. Continuous measurement of nitrate concentration in a highly event-responsive agricultural catchment in south-west of France: is the gain of information useful? Hydrol. Process. 27 (12), 1751–1763. http://dx.doi.org/10.1002/hyp.9324.
Garcia-Pintado, J., Neal, J.C., Mason, D.C., Dance, S.L., Bates, P.D., 2013. Scheduling satellite-based SAR acquisition for sequential assimilation of water level observations into flood modelling. J. Hydrol. 495, 252–266. http://dx.doi.org/10.1016/j.jhydrol.2013.03.050.
Gellis, A.C., 2013. Factors influencing storm-generated suspended-sediment concentrations and loads in four basins of contrasting land use, humid-tropical Puerto Rico. Catena 104, 39–57. http://dx.doi.org/10.1016/j.catena.2012.10.018.
Grayson, R.B., Finlayson, B.L., Gippel, C.J., Hart, B.T., 1996. The potential of field turbidity measurements for the computation of total phosphorus and suspended solids loads. J. Environ. Manag. 47 (3), 257–267. http://dx.doi.org/10.1006/jema.1996.0051.
Heathwaite, A.L., Johnes, P.J., 1996. Contribution of nitrogen species and phosphorus fractions to stream water quality in agricultural catchments. Hydrol. Process. 10 (7), 971–983. http://dx.doi.org/10.1002/(sici)1099-1085(199607)10:7<971::aid-hyp351>3.0.co;2-n.
Hendrickson, G.E., Krieger, R.A., 1964. Geochemistry of Natural Waters of the Blue Grass Region (Kentucky).
House, W.A., Denison, F.H., 1997. Nutrient dynamics in a lowland stream impacted by sewage effluent: Great Ouse, England. Sci. Total Environ. 205 (1), 25–49. http://dx.doi.org/10.1016/s0048-9697(97)00086-7.
House, W.A., Warwick, M.S., 1998. Hysteresis of the solute concentration/discharge relationship in rivers during storms. Water Res. 32 (8), 2279–2290. http://dx.doi.org/10.1016/s0043-1354(97)00473-9.
Huebsch, M., et al., 2014. Mobilisation or dilution? Nitrate response of karst springs to high rainfall events. Hydrol. Earth Syst. Sci. 18 (11), 4423–4435. http://dx.doi.org/10.5194/hess-18-4423-2014.
ISO 1088, 2007. Hydrometry – Velocity-area Methods Using Current-Meters – Collection and Processing of Data for Determination of Uncertainties in Flow Measurement. ISO Standards.
ISO 1100-2, 2010. Hydrometry – Measurement of Liquid Flow in Open Channels – Part 2: Determination of the Stage-discharge Relationship. ISO Standards.
Jarvie, H.P., et al., 2005. Role of river bed sediments as sources and sinks of phosphorus across two major eutrophic UK river basins: the Hampshire Avon and Herefordshire wye. J. Hydrol. 304 (1–4), 51–74. http://dx.doi.org/10.1016/j.jhydrol.2004.10.002.
Jarvie, H.P., et al., 2002. Phosphorus sources, speciation and dynamics in the lowland eutrophic River Kennet, UK. Sci. Total Environ. 282, 175–203. http://dx.doi.org/10.1016/s0048-9697(01)00951-2.
Jiang, R., et al., 2010. Hydrological process controls on nitrogen export during storm events in an agricultural watershed. Soil Sci. Plant Nutr. 56 (1), 72–85. http://dx.doi.org/10.1111/j.1747-0765.2010.00456.x.
Jordan, P., Arnscheidt, A., McGrogan, H., McCormick, S., 2007. Characterising phosphorus transfers in rural catchments using a continuous bank-side analyser. Hydrol. Earth Syst. Sci. 11 (1), 372–381.
Kronvang, B., Laubel, A., Grant, R., 1997. Suspended sediment and particulate phosphorus transport and delivery pathways in an arable catchment, Gelbaek Stream, Denmark. Hydrol. Process. 11 (6), 627–642. http://dx.doi.org/10.1002/(sici)1099-1085(199705)11:6<627::aid-hyp481>3.0.co;2-e.
Krueger, T., et al., 2009. Uncertainties in data and models to describe event dynamics of agricultural sediment and phosphorus transfer. J. Environ. Qual. 38 (3), 1137–1148. http://dx.doi.org/10.2134/jeq2008.0179.
Langlois, J.L., Johnson, D.W., Mehuys, G.R., 2005. Suspended sediment dynamics associated with snowmelt runoff in a small mountain stream of Lake Tahoe (Nevada). Hydrol. Process. 19 (18), 3569–3580. http://dx.doi.org/10.1002/hyp.5844.
Lawler, D.M., Petts, G.E., Foster, I.D.L., Harper, S., 2006. Turbidity dynamics during spring storm events in an urban headwater river system: the Upper Tame, West Midlands, UK. Sci. Total Environ. 360 (1–3), 109–126. http://dx.doi.org/10.1016/j.scitotenv.2005.08.032.
Littlewood, I.G., 1992. Estimating Contaminant Loads in Rivers: A Review. Institute of Hydrology, Wallingford.
Lloyd, C.E.M., Freer, J.E., Johnes, P.J., Collins, A.L., 2015a. Technical note: testing an improved index for analysing storm nutrient hysteresis. Hydrol. Earth Syst. Sci. Discuss. 12 (8), 7875–7892. http://dx.doi.org/10.5194/hessd-12-7875-2015.
Lloyd, C.E.M., Freer, J.E., Johnes, P.J., Coxon, G., Collins, A.L., 2015b. Discharge and nutrient uncertainty: implications for nutrient flux estimation in small streams. Hydrological Processes http://dx.doi.org/10.1002/hyp.10574 (n/a-n/a).
McGonigle, D.F., et al., 2014. Developing demonstration test catchments as a platform for transdisciplinary land management research in England and Wales. Environmental Science: Processes & Impacts 16, 1618–1628. http://dx.doi.org/10.1039/C3EM00658A.
Meade, R., Parker, R., 1985. Sediments in Rivers of the United States.
Nord, G., et al., 2014. Applicability of acoustic Doppler devices for flow velocity measurements and discharge estimation in flows with sediment transport. J. Hydrol. 509, 504–518. http://dx.doi.org/10.1016/j.jhydrol.2013.11.020.
Novotny, V., 1980. Delivery of suspended sediment and pollutants from nonpoint sources during overland flow. Water Resour. Bull. 16 (6), 1057–1065.
Outram, F.N., et al., 2014. High-frequency monitoring of nitrogen and phosphorus response in three rural catchments to the end of the 2011–2012 drought in England. Hydrol. Earth Syst. Sci. 18 (9), 3429–3448. http://dx.doi.org/10.5194/hess-18-3429-2014.

Prior, H., Johnes, P.J., 2002. Regulation of surface water quality in a Cretaceous Chalk catchment, UK: an assessment of the relative importance of instream and wetland processes. Sci. Total Environ. 282, 159–174. http://dx.doi.org/10.1016/s0048-9697(01)00950-0.

Ramos, T.B., et al., 2015. Sediment and nutrient dynamics during storm events in the Enxoe temporary river, southern Portugal. Catena 127, 177–190. http://dx.doi.org/10.1016/j.catena.2015.01.001.

Robson, A., Reed, D., 1999. Flood Estimation Handbook — FEH CD-ROM 3. Institute of Hydrology, Wallingford.

Saxton, K.E., Lenz, A.T., 1967. Antecedent retention indexes predict soil moisture. Journal of the Hydraulics Division-Asce 93, 223–241.

Stubblefield, A.P., Reuter, J.E., Dahlgren, R.A., Goldman, C.R., 2007. Use of turbidometry to characterize suspended sediment and phosphorus fluxes in the Lake Tahoe basin, California, USA. Hydrol. Process. 21 (3), 281–291. http://dx.doi.org/10.1002/hyp.6234.

Toler, L.G., Ocala, F., 1965. Relation between chemical quality and water discharge in Spring Creek, Southwestern Georgia. U.S. Geol. Surv. Prof. Pap. 525 (3–4), C209–C213.

Verhoff, F.H., Melfi, D.A., Yaksich, S.M., 1979. Storm travel distance calculations for total phosphorus and suspended materials in rivers. Water Resour. Res. 15 (6), 1354–1360. http://dx.doi.org/10.1029/WR015i006p01354.

Walling, D.E., Amos, C.M., 1999. Source, storage and mobilisation of fine sediment in a chalk stream system. Hydrol. Process. 13 (3), 323–340. http://dx.doi.org/10.1002/(sici)1099-1085(19990228)13:3<323::aid-hyp741>3.0.co;2-k.

Walling, D.E., Collins, A.L., Stroud, R.W., 2008. Tracing suspended sediment and particulate phosphorus sources in catchments. J. Hydrol. 350 (3–4), 274–289. http://dx.doi.org/10.1016/j.jhydrol.2007.10.047.

Walling, D.E., et al., 2003. Storage of sediment-associated nutrients and contaminants in river channel and floodplain systems. Appl. Geochem. 18 (2), 195–220. http://dx.doi.org/10.1016/s0883-2927(02)00121-x.

Walling, D.E., Webb, B.W., 1987. Suspended load in gravel-bed rivers: UK experience. In: Thorne, C.R., Bathurst, J.C., Hey, D.L. (Eds.), Sediment Transport in Gravel-bed Rivers. Wiley, pp. 691–732.

Webb, B.W., Walling, D.E., 1985. Nitrate behavior in streamflow from a grassland catchment in Devon, UK. Water Res. 19 (8), 1005–1016. http://dx.doi.org/10.1016/0043-1354(85)90369-0.

Williams, G.P., 1989. Sediment concentration versus water discharge during single hydrologic events in rivers. J. Hydrol. 111 (1–4), 89–106. http://dx.doi.org/10.1016/0022-1694(89)90254-0.

Wood, P.A., 1977. Controls of variation in suspended sediment concentration in River Rother, West Sussex, England. Sedimentology 24 (3), 437–445. http://dx.doi.org/10.1111/j.1365-3091.1977.tb00131.x.

Yates, C.A., Johnes, P.J., 2013. Nitrogen speciation and phosphorus fractionation dynamics in a lowland chalk catchment. Sci. Total Environ. 444, 466–479. http://dx.doi.org/10.1016/j.scitotenv.2012.12.002.

Zhang, Y., Collins, A.L., Gooday, R.D., 2012. Application of the FARMSCOPER tool for assessing agricultural diffuse pollution mitigation methods across the Hampshire Avon Demonstration Test Catchment, UK. Environ. Sci. Pol. 24, 120–131. http://dx.doi.org/10.1016/j.envsci.2012.08.003.